

## Article

# Waste SMD LEDs from End-of-Life Residential LED Lamps: Presence and Characterisation of Rare Earth Elements and Precious Metals as a Function of Correlated Colour Temperature

Konstantinos M. Sideris <sup>1,2,\*</sup>, Ioannis Katsiris <sup>2</sup>, Dimitrios Fragkoulis <sup>3</sup>, Vassilis N. Stathopoulos <sup>3</sup>   
and Panagiotis Sinioros <sup>1</sup>

<sup>1</sup> Department of Electrical & Electronic Engineering, University of West Attica, 122 44 Egaleo, Greece; sinioros@uniwa.gr

<sup>2</sup> Department of Electrical and Electronic Engineering Educators, School of Pedagogical and Technological Education, 151 22 Marousi Attica, Greece; ikatsiris@aspete.gr

<sup>3</sup> Department of Agricultural Development, Agrifood and Natural Resources Management, National and Kapodistrian University of Athens, Psachna Campus, 344 00 Evia, Greece; dimifragkoulis@uoa.gr (D.F.); vasta@uoa.gr (V.N.S.)

\* Correspondence: ksideris@uniwa.gr

**Abstract:** Energy consumption in buildings is linked to lighting technology. Light-emitting diode (LED) technology includes lamps and luminaires for general lighting applications. Due to their structure, LED lamps are expected to generate specific waste electrical and electronic equipment (WEEE) streams. LEDs are the main source of luminous flux, and their elemental composition is of particular interest to the recycling sector. In this study, surface-mount device (SMD) LEDs from six types of LED lamps (E27, E14, G9, R7S, GU10, and MR16) were removed, collected, separated by correlated colour temperature (CCT) (2700 K, 3000 K, 4000 K, and 6500 K), and characterised for the presence of rare earth elements and precious metals. They were digested with HNO<sub>3</sub>, aqua regia, and HF in a hot plate and characterised by inductively coupled plasma mass spectrometry (ICP-MS). The concentration of each element as a function of CCT ranged as follows: lanthanum, 242–1840 mg/kg; cerium, 132–284 mg/kg; europium, 15–69 mg/kg; gadolinium, 1.9–3.8 mg/kg; terbium, 0.1–0.4 mg/kg; lutetium, 29–6381 mg/kg; yttrium, 4804–11,551 mg/kg; silver, 2712–5262 mg/kg; gold, 502–956 mg/kg; and palladium, 32–110 mg/kg. These results indicate the need for selective removal and separate recycling processes of SMD LEDs from LED lamps.

**Keywords:** measurements and characterisation; LED lamps; LED module; SMD LEDs; rare earth elements; precious metals; ICP-MS analysis



**Citation:** Sideris, K.M.; Katsiris, I.; Fragkoulis, D.; Stathopoulos, V.N.; Sinioros, P. Waste SMD LEDs from End-of-Life Residential LED Lamps: Presence and Characterisation of Rare Earth Elements and Precious Metals as a Function of Correlated Colour Temperature. *Recycling* **2024**, *9*, 128. <https://doi.org/10.3390/recycling9060128>

Academic Editor: Jack Groppo

Received: 31 October 2024

Revised: 17 December 2024

Accepted: 19 December 2024

Published: 21 December 2024



**Copyright:** © 2024 by the authors. Licensee MDPI, Basel, Switzerland. This article is an open access article distributed under the terms and conditions of the Creative Commons Attribution (CC BY) license (<https://creativecommons.org/licenses/by/4.0/>).

## 1. Introduction

The generation of waste electrical and electronic equipment (WEEE) has exponentially increased in recent years. This raises concerns regarding how to tackle this problem and, particularly, how to improve its management. Management begins with consumer awareness of the circular economy and ends with efforts to recover and recycle raw materials previously used to manufacture these devices [1]. However, the production of these appliances is constantly increasing (annual growth of approximately 5%) [2] while their lifespan is decreasing, resulting in the depletion of reserves of these metals in the Earth's crust, making their conservation a matter of particular concern [3,4]. Environmental protection is linked to the consumption of electricity, the protection of reserves, air pollutants, and the deposit of waste in the Earth's crust [5].

The circular economy and WEEE recycling can support these factors in two ways. First, in reducing the energy and water used in the stages from natural extraction to raw material production, recovering metals from WEEE can save up to 85–90% of the energy required

to extract them from natural mines [6,7]. Both energy and water consumption and the environmental footprint of their production are functions of each metal [7], which creates more incentives for mapping critical raw materials and metals of high economic value on WEEE to achieve their targeted recycling [8]. Second, they prevent the uncontrolled deposition of toxic elements in the Earth's crust [9], since the circular economy aims to minimise the amount of WEEE landfilled and, because of this limitation, follows a priority order of elimination, reduction, reuse, and recycling, with any remaining waste disposed of in an environmentally sound and controlled manner [10].

Therefore, WEEE is a valuable secondary source of specific materials and elements, such as rare earth elements (REEs) and precious metals (PMs), which can contribute to the balance between reserves and demand, especially for metals classified as critical, as the concentration of metals in WEEE is higher than that found in the Earth's crust [11]. Rare earth elements and precious metals have been and continue to be widely used in electrical and electronic equipment due to their exceptional properties [12,13].

Rare earth elements are a group of 17 metallic elements in the periodic table, including the Lanthanide series (lanthanum (La) to lutetium (Lu)), scandium (Sc), and yttrium (Y). Scandium and yttrium are included in the REEs because of their similar physico-chemical properties and tendency to occur in the same ores. Precious metals include the platinum group metals (PGMs), gold (Au), and silver (Ag) [14,15].

Efforts to recover and recycle metals for sustainability make the management of WEEE a crucial factor. The pre-treatment phase is a critical stage of recycling, during which the concentrations of metals classified as critical or of high economic interest can vary significantly [16,17]. To increase the recovery efficiency of rare earth elements, precious metals, and critical raw materials (CRMs) from WEEE, it is necessary to separate their structures [18,19]. It is critical to consider separation during the pre-treatment stage, as this can significantly affect the retention or loss of the aforementioned metals, especially in cases where concentrations are low [20]. To further improve the level of recovery, it may be helpful to remove or cut out specific parts of their individual structures that have high concentrations of specific metals. This is typical for PMs (such as electrical contacts, electrodes, and electrical interconnects), but not usually for REEs, which are used in a variety of applications (such as phosphors and ceramics) with a diffuse presence in the individual structures of the device [21].

The categorisation of WEEE varies among different regulations and directives in different countries or continents [22]. According to the European Union Directive 2012/19/EU [23], WEEE is divided into six categories. Each category consists of several types of equipment. Category 3 covers lamps and, in particular, lamp technologies: (a) high-intensity discharge (HID), (b) fluorescent, and (c) light-emitting diode (LED). Each subcategory of the above technologies includes different types of lamps, which may vary in size, application, and electrical and photometric characteristics. It is important to note that, LED lamps that have reached the end of their functional life may be classified as hazardous WEEE, especially if they are grouped with fluorescent lamps at recycling collection points, because of the risk of contamination by mercury (Hg) contained in fluorescent lamps. Therefore, a separate collection of lamps based on their operating principles is required [24].

Light-emitting diode lamps are solid-state energy converters. In the design and manufacturing process of LED lamps, many simple or more complex raw materials are used, some of which (toxic heavy metals) can harm both the environment and humans during the lamp manufacturing process. Therefore, the "green design" of electrical and electronic equipment (EEE) and "design for environment" are excellent parameters for EEE design and WEEE recycling [25]. LED lamps are up to 95% recyclable, but their complex construction requires the disassembly and separation of individual structures and components to be sent to separate recycling streams [19]. LED lamps are a new type of electronic waste for which there are currently no standardised recycling processes [26]. As the name of the technology suggests, these lamps use LEDs of different technologies and photometric parameters to generate luminous flux. The use of LEDs to generate luminous flux offers

significant advantages over the two older lighting technologies, incandescent and fluorescent, relating to (a) the ease with which their geometric dimensions can be adapted to the challenges posed by the requirements of each lighting application [27], (b) their reduced heat generation, (c) their improved efficiency (lm/W), and (d) the absence of mercury in their structure, making them safer both for the environment and for workers in recycling plants [28,29]. LEDs are classified as WEEE under the European Union Directive 2012/19/EU [23]. Surface-mount device (SMD) LEDs are particularly interesting e-components for targeted recycling because of the presence of rare earth elements and precious metals in their structure [30], with the concentrations of these metals varying as a function of their correlated colour temperature [31].

The collection, management, and recovery of the stored potential of the materials used in the manufacture of lamps contributes to the implementation of the concept of “urban mining”, the protection of the environment through natural reserves by reducing mining [32], as well as elements hazardous to humans and the environment, such as various flame-retardant substrates, and elements such as lead and arsenic [33,34]. A balance between the content, price, and criticality of these materials determines the viability of “urban mines” and recycling plants [35]. To achieve the above, characterisation results are needed for (a) the total and individual masses of LED lamps, (b) the localisation of the above metals in their structure, (c) their concentrations per component type, and (d) the modulation of their concentrations at the device level.

### 1.1. LED Lamps

To achieve zero-energy buildings (ZEBs) or, more realistically, near-zero energy buildings (n-ZEBs), it is considered necessary to reduce the electricity consumption in buildings. To this end, LED lamps were introduced in 2010 to replace the incandescent and fluorescent technologies used for residential lighting because of their significant advantages over the above technologies [36–38]. Compared with previous lighting technologies, LED lamps convert electrical energy into visible light more efficiently and with a faster response time (on/off switching at the ms level) [39–41], making them a safer and more environmentally friendly technology [42–45]. Their more efficient operation is expected to reduce the share of global electricity consumption corresponding to artificial lighting [39,46] (18–21%), of which a significant portion (8%) is consumed in residential buildings [40,47], thus contributing to the reduction in carbon emissions (10%) corresponding to the production of the electricity mentioned above [28,33,41,48]. The proper management of artificial lighting is not limited to the context of electricity consumption. However, it extends to the collection and management of this specific WEEE, setting objectives, among others, related to the management of hazardous substances contained in the lamps and the study of (a) the re-use of their structures and components [40,47], and (b) the possibility of recovering elements of the periodic table, either accompanied by a high economic value or classification as CRMs.

LED lamps (Figure 1) are more complex in design than previous lighting technologies [49]. It is worth noting that 96 simple or more complex raw materials [25,50], including REEs and PMs, are used in the design and manufacturing processes of LED lamps and are located in their specific structures, such as (a) LED modules and surface-mount device (SMD) LEDs (Figure 1(a1)), (b) filament LEDs (Figure 1b), and (c) chip-on-board (COB) LEDs (Figure 1c), as well as in the structures required for their operation (drivers) (Figure 1(a2,b1)), depending on the LED technology used by each type of lamp [30,51]. The presence of these metal categories in LED lamps, the high market share of LEDs in the building lighting sector compared to other sectors such as automotive lighting, landscape lighting, display, backlighting applications, signalling, and guidance, and the high level of recovery of these metal make this type of WEEE a significant and highly concentrated secondary source for the recovery of valuable and critical raw materials [19,21,33,52–54].

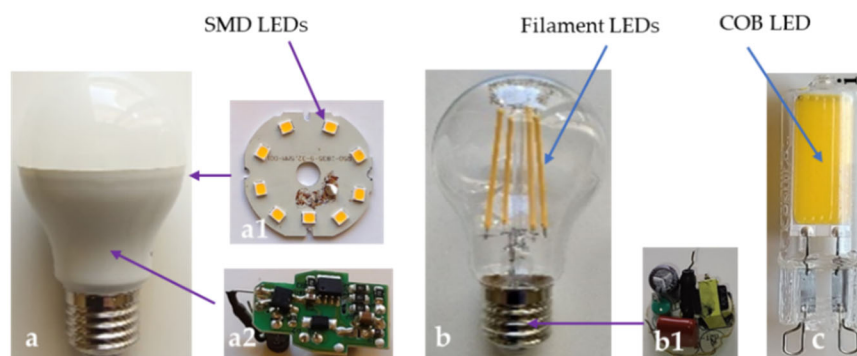


**Figure 1.** (a) LED lamps with SMD LEDs, (a1) LED module, (a2) driver, (b) LED lamps with filament LEDs, (b1) driver, and (c) LED lamps with COB LED (retro style) (authors' images).

Where economically viable, LED lamps should be disassembled into their structures. Their components should be released for more efficient management during lamp recycling, which can be achieved in several stages. In the first stage, LED lamps can be dismantled by producing the following mass fractions or parts thereof, depending on their type and construction: (a) metals, (b) plastics, (c) glass, (d) ceramics, (e) drivers, (f) LED modules, and (g) filament LEDs. In the second stage, drivers can be separated into their electronic components and bare printed circuit boards (PCBs), whereas the LED module can be separated into its SMD LEDs and a bare LED module. Any hazardous components requiring special handling, such as the driver's electrolytic capacitors, can be removed at this stage. The separation of structures and components based on functionality is not applicable unless power surges cause premature damage to the lamp. The selective removal of high-economic-interest components can also be applied after lamp separation. For example, in the case of LEDs, extracting and creating simple compositions and high-concentration streams is essential to reduce losses and improve the recovery rate of valuable and critical raw materials. This supports the sustainability of recycling facilities and helps achieve the best possible balance between the economic benefits of recycling and the environmental impacts of recycling processes [20,24,54–61]. As an indication, Appendix A, Figure A1 shows a detailed average percentage analysis of the individual components of the most common LED lamp used in residential lighting applications (E27-C Classic—A60) in relation to the total mass of the lamp.

### 1.2. SMD LEDs

LEDs are static electricity converters manufactured using microelectronic technology [39] adapted to the specific technological challenges of their operation in terms of the radiation they emit and the management of the heat generated [27,62,63]. Unlike for the heated filament of incandescent lamps and microlamps [64], their operation is based on the spontaneous emission of radiation from the recombination of redundant holes and electrons as a result of the potential difference and the flow of electric current when they are correctly polarised [65]. Depending on the radiation emitted, and, in particular, the dominant emission wavelength, LEDs can be classified as ultraviolet LEDs (UV-LEDs), <380 nm; visible LEDs (V-LEDs), 380–780 nm; and infrared LEDs (IR-LEDs), >780 nm [66]. When LEDs are used, in general, or specific lighting applications, their structures are designed to convert electrical energy into light radiation. LEDs began their commercial presence in the 1960s, usually as indicator lights, but their substantial presence in the lighting sector began in 2014 with the discovery of the “blue LED” [67].

Various types of SMD white LEDs are used in lighting applications, such as general lighting lamps, display lighting, and other technological applications where luminous flux is required [68,69]. Their use is associated with the following advantages: (a) energy efficiency [69], (b) photometric characteristics and a fast response [70], (c) a long operating life [69], (d) the absence of mercury [69], and (e) being soldered in predetermined positions on printed circuit boards for various technological applications [71] according to the desired

polar distribution of the luminous flux. The external dimensions of their structure determine their types. For example, type 2835 has dimensions of 2.8 mm (h)  $\times$  3.5 mm (w), while type 3528 has dimensions of 3.5 mm (h)  $\times$  2.8 mm (w).

An SMD LED (Figure 2a) consists of several structures, each of which can be made of different materials depending on the application [27,30]. From base to top, an SMD LED consists of the following individual functional structures: (a) lead frame—external power supply contacts (Figure 2b); (b) moulding component—plastic case (Figure 2b); (c) die's substrate (rear view) (Figure 2c); (d) LED dies (top view)—structure for generating electromagnetic radiation (Figure 2d); and (e) silicone or epoxy resin containing phosphor (Figure 2e) [72–74]. According to Hamidnia et al. (2018) and Alim et al. (2021), sapphire, silicon carbide, and silicon have been used as substrate materials for LED chips in the production of SMD LEDs, selected according to the economic criteria for each LED application [27,63]. According to Marwede et al. (2012) and Nikulski et al. (2021), the concentrations of CRMs and PMs in SMD LEDs can be expressed as a function of the surface area of the dies (mg/kg per 1 mm<sup>2</sup>) [75,76]. According to Marwede et al. (2012) [75], Cenci, Dal Berto, and Schneider et al. (2020) [77], and Nikulski et al. (2021) [76], there is a significant difference in the total die area per LED lighting product depending on the lighting application.

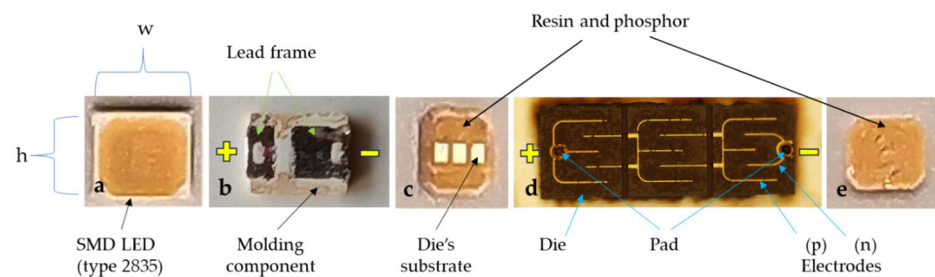


**Figure 2.** Structure analysis of an SMD LED 2835 (authors' images). (a) upper face of the whole structure, (b) back view, (c) die's substrate, (d) electrical structure of dies, (e) resin containing phosphorus.

Except for the flip-chip structure, conductive wires were used for the electrical supply of the dies [63]. The wire bonding process is a critical parameter of the overall LED structure. It aims to transfer the electrical energy to the die(s) by connecting their electrical contacts (pads) to the external contacts of the package (lead frame), as in the case of integrated circuits [27,69] using microelectronic technology (wire border) [27,78]. In general, microelectronic technology uses different types of conducting wires, such as (a) single structures (solid), (b) alloys, and (c) overlays (superimposed layers) (e.g., Cu—Pd [63,79], Ag—Pd [63]). In the manufacture of their various types, base and precious metals are used to address challenges [80] related to electrical and thermal conductivity, mechanical strength, performance, and manufacturing cost. To meet these challenges [81], precious metals such as silver, palladium, and gold have been used to produce “palladium-coated copper wire with a flash-gold layer” (PCA) [82], Pd-coated Cu wires [80,83], and Ni-coated Cu wires [83]. When selecting the type and composition of the wire, the following parameters of SMD LEDs are taken into account, among others: (a) the construction material of the die pads [63,78], the correlated colour temperature (CCT) [63,84], and the warranty time for good operation [85]. To reduce the cost of manufacturing SMD LEDs, wires with a reduced gold content of 20–40% and an increased silver content are used, taking advantage of the significant difference in the commercial price of these two metals to create silver alloy (Ag alloy) wires [84]. All three types of wires are used in LEDs, in particular (a) solids [85,86] Au, Ag, and Cu; (b) alloys [85,86]; and (c) coated wires (gold-coated silver bonding wire [87]; Pd-coated copper bonding wire [87]; Ag (96%) as base, Pd (3%) as palladium coating, and Au (1%) as gold flash [88]; Ag, Au (8–30%), and Pd (0.01–6%) [63,89]).

### 1.2.1. Production of Visible Radiation (“White Light”)

The production of “white light” for general or specific lighting applications can be achieved using different manufacturing combinations of LED structures [90]. The first combination requires the precise synthesis of the phosphors of the three basic colours, namely red (R), green (G), and blue (B), excited by the radiation of a specific wavelength or region of the electromagnetic spectrum (usually near ultraviolet) [91], most commonly produced by independent semiconductor structures of LEDs (dies) [92,93]. The generation of “white light” by this synergy is characteristically referred to as a “colour-mixing white LED” (CMW-LED) [94]. The second and currently most common technological combination for producing white light is the combination of one or more semiconductor structures emitting in the “cold” region of the visible part of the electromagnetic spectrum (455 nm) with the presence and excitation of a yellow phosphor [63,90]. This optical/material synergy, characteristically called a “Phosphor-Converted White LED” (PC-WLED), contributes to its emission spectrum [28,63,95–97]. The high energy efficiency of this technology makes LED structures suitable for use in artificial lighting applications (i.e., lamps and luminaires) [98].

White LEDs are the fourth generation of solid-state lighting (SSL) devices with the advantages of high luminous efficacy (lm/W) and long life. In combining the above advantages, white LEDs are generally considered more environmentally friendly, helping reduce carbon emissions and conserve natural resources [29]. However, an essential challenge in designing LEDs for optimal use is improving some of their photometric parameters, such as the correlated colour temperature and colour rendering index (CRI) [99]. For example, yellow phosphors, due to the absence of “warm” wavelengths, produce correlated colour temperatures  $\geq 4500$  K accompanied by a low colour rendering index and do not meet the photometric requirements of the room in most artificial lighting applications [45,46,90,100]. The technological shift in the CCT of the luminous flux, from “cool” to “warm” wavelengths, can be achieved by various technological combinations while keeping the same excitation radiation of the phosphors (near UV or “blue LED”) per application case [101], such as through (a) the use of resins of appropriate composition and variable thickness, enriched with the appropriate phosphor impurities and concentrations for each application, and (b) resin layers with the appropriate yellow and red phosphor impurities to meet the photometric requirements specified for each artificial lighting application [45,65,92,101,102].

### 1.2.2. Presence of REEs in Inorganic Phosphors

The participation of REEs in the inorganic phosphors used in the production of SMD LEDs modulates the parameters of SMD LEDs in terms of their functional stability, luminous efficiency (lm/W), CRI, and CCT, thus meeting the requirements of each lighting application [29,91,103]. In general, inorganic phosphors are composed of a “host lattice” and “activator(s)” [104,105]. The presence of REEs in the chemical types of inorganic phosphors is associated either with their participation in the host lattice or with their low participation ( $\sim 1$  mol%) as activators [106], while their dual presence (host lattice and activator) is not excluded [107]. As mentioned previously, the presence of REEs in inorganic phosphors modulates their emission spectra. The emission spectrum of LEDs for lighting applications is an optical mixture of the radiation produced by phosphor excitation diode(s) and the radiation produced during phosphor de-excitation [100,108–110]. The contribution of these two types of visible radiations to the luminous flux of LEDs determines their important photometric parameters, such as CCT and CRI [65,111]. For the precise synthesis of the generated radiation and the wide range of LEDs, more than one rare-earth ion (up to three) can be used as phosphor activators (dopant and co-dopant) [99,104], whose ratios and concentrations cooperate in the desired modulation of their luminous flux [112], because each rare-earth ion contributes differently to its modulation [92,109,112].

### 1.3. SMD LEDs—A Special Type of WEEE

From a recycling point of view, SMD LEDs are particularly interesting because of the presence and concentration of REEs and PMs in their structure [30]. Of particular

interest, however, is the fact that this surface-mounted electrical component modulates the presence of REEs in LED lamps to a high percentage or exclusively as a function of the presence or absence of multi-layer ceramic capacitors (MLCCs) in their structure because this type of capacitor, like LEDs, contains REEs [20,61,113]. According to Sideris et al. (2023), MLCCs are not consistently present in the drivers of most of the lamp types examined [61]. According to Charles et al. (2020) [20] and Xia et al. (2024) [113], other electrical and electronic components contained in drivers (typical design), such as transistors, tantalum (Ta) capacitors, electrolytic capacitors, resistors, inductors, integrated circuits, diodes, piezoelectrics, crystals, resonators, sockets, pin terminals, heat sinks, and bare boards, do not contain REEs in their structures. According to Cenci, Dal Berto, and Schneider et al. (2020) [77] and Cenci, Dal Berto, and Castillo et al. (2020) [51], the presence of REEs in the LED lamps they studied was essentially related to the presence of LEDs. In general, the structure of lamp drivers is a function of both the design technology and electrical power of the lamps. These two parameters are of particular interest from both the recycling point of view (stored potential of REEs and PMs) and from the point of view of electrical power quality (lamp power factor) [114]. Based on the above, it is clear that the presence of REEs in the structure of LED lamps for residential applications is linked to the presence of SMD LEDs.

#### Characterisation of SMD LEDs for the Presence of REEs and PMs—Literature Review

Light-emitting diode lamps are a new technology for lighting buildings. The use of LED lamps with SMD LEDs started from an extremely low penetration rate in 2010 to 100% of the market by 2025. When considering that (a) there are not many relevant studies on their recycling due to their short presence and long lifetime, (b) they have a more complex structure than the previous technologies, (c) a large number of raw materials are used in the production of LED lamps [50], many of which are accompanied by supply risk (SR) and economic importance (EI) indicators [53], and (d) the recycling of their units, such as SMD LEDs, is directed to specialised recycling plants, it seems appropriate to divide the characterisation of the structures and their components in order to provide targeted data that will contribute to a better design of their recycling (separation) and a more efficient recovery of CRMs and valuable elements, such as REEs and PMs [73,77,113,115–117].

The following is a list of studies relevant to the characterisation of this specific type of WEEE. Zhan et al. (2015) presented characterisation results for the structure and dies of SMD LEDs, which are affected by the presence of PMs (Au) [118]. Dodbiba et al. (2019) conducted a study using an E27-type LED lamp with a power of 30 W. The study provided results on the percentages of lamp structures, including the driver and the LED module. In addition, they reported characterisation results related to the structure of SMD LEDs (type 5050) from the E27 lamp owing to the presence of PMs (Ag, Au) and REEs (Y) [119]. Cenci, Dal Berto, and Schneider et al. (2020) characterised SMD LEDs from LED lamps (tube and E27) and presented results for the concentrations of base metals, technological metals, REEs, and PMs in relation to the driver, LED modules, and SMD LEDs [77]. Zhan et al. (2020) presented the results of the characterisation of the structure of SMD LEDs (type 3528) affected by the presence of PMs (Ag) [120]. Cenci, Dal Berto, and Castillo et al. (2020) studied four groups of LED lamps, including L1 (T12 tube) and L2–L4 (bulbs) (E27). Each group of ten lamps corresponded to a different manufacturer. The researchers reported the characterisation results for REEs (Y, Ce) and PMs (Ag, Au). The characterisation results included drivers, bare LED modules, and SMD LEDs contained in the aforementioned lamps [51]. Oliveira et al. (2020) presented the results of their study on the structural characterisation of SMD LEDs (type 2835) in the presence of REEs (Y, Ce, Gd) and PMs (Ag) [73]. Balinski et al. (2022) conducted a study of 100 LED lamps with Edison lamp bases. The lamps were separated into five basic structures, including the LED modules and drivers. The authors presented results from the characterisation of dies and encapsulation from SMD LEDs for the presence of REEs (Y, Eu, Gd), PMs (Pd, Ag, Au), and other elements from the periodic table [30]. Vinhal et al. (2022) presented the results of their study on

the structural characterisation of SMD LEDs (type 2835), “cool white” (CW) and “warm white” (WW) from LED tube lamps with respect to the presence of REEs (Y, Ce) and PMs (Ag, Au) [31]. Pourhossein et al. (2022) studied end-of-life LEDs. Among other results, they presented data on the presence of PMs (Ag, Au) in their structure [26]. Mandal et al. (2023) presented data on the potential of valuable metals in LEDs of different types and technologies, particularly for REEs (Y, Ce, and Gd) and PMs (Au, Ag) [121]. Illés and Kékesi (2023) investigated four different E27-C lamps for professional lighting applications and presented results for SMD LEDs in terms of the presence of REEs (Ce, Eu and Y) and PMs (Ag, Au) [122]. Zheng et al. (2024) investigated SMD LEDs (type 3528) from “strip lights”. Among other results, they presented data on PMs (Ag) [34]. The structure of the various types of SMD LEDs and the mapping of the critical, technological, and valuable materials have been extensively studied and successfully presented in a number of studies, including the following: Tang et al. (2017) [62], Zhang et al. (2018) [123], Zhan et al. (2020) [120], Martins, Tanabe, and Bertuol (2020) [124], Cenci et al. (2020) [51], Zhang, Zhan, and Xu (2021) [125], Vinhal et al. (2022) [31], and Illés and Kékesi (2023) [122].

Based on the above, in considering that LEDs are WEEE and taking a more realistic approach from the recycling side, this study presents the following novelties: (a) the study of six different types of residential LED lamps (E27, E14, G9, R7S, GU10, and MR16) in terms of the mass content and type of SMD LEDs; (b) the characterisation of the collected SMD LEDs according to the correlated colour temperature and, in particular, for four similar cases based on 2700 K, 3000 K, 4000 K, and 6500 K, concerning the presence of REEs and PMs; (c) the conditional characterisation of the types mentioned above of LED lamps concerning the REEs content in their structure; and (d) the conditional calculation of the stored potential of the PMs in the SMD LEDs of each of the above-mentioned types of lamps.

## 2. Materials and Methods

A random sample and a selectively enriched sample of LED lamps were examined. The random sample was provided by “AEGEAN RECYCLING-FOUNDRIES SA”.

The methodological approach used in this study included five stages: (1) the collection and separation of LED lamps, (2) disassembly and testing, (3) sample preparation and analysis by inductively coupled plasma mass spectrometry (ICP-MS), and (4) the calculation of the stored potential of the PMs in the lamps’ SMD LEDs and characterisation of the lamps in terms of REEs. All measurements were repeated three times under the same conditions, and the results were averaged.

### 2.1. Collection and Separation

This stage consisted of (a) the collection, integrity check, cleaning, weighing, counting, and separation of lamps by base type (i.e., E27) and LED type (SMD, filament, and COB); and (b) the selection of unique lamps based on their electrical and photometric characteristics and brand, in order to generate innovative data on the lamps to be recycled according to users’ preferences.

### 2.2. Disassembly and Testing

This stage involved the (a) manual disassembly of the unique lamps, (b) removal and dismantling of the LED modules, (c) weighing and counting of the individual masses and their correlation with the total and individual masses of the structures and components, and (d) recording of the number and dimensions (type) of SMD LEDs.

The following equipment was used for the implementation of this stage: basic and special tools such as tweezers, hot-air-gun-rated temperature (brand: BOSCH; (Robert Bosch GmbH, Stuttgart, Germany) model: GHG 20-60), calibrated thickness gauge (brand: UNIOR; (UNIOR Kovaška industrija d.d., Zreče, Slovenia) model: 271), calibrated micrometre (brand: INSIZE; (INSIZE Co., Ltd., Suzhou, China) model: 3210-25A), and precision balance (brand: KERN; (KERN & SOHN GmbH, Balingen, Germany) EWJ-300-3,  $d = 0.001$  g).

### 2.3. Sample Preparation and ICP-MS Analysis

This phase aimed to generate innovative data on SMD LEDs, particularly on the concentrations of rare earth elements and precious metals in the collected waste of SMD LEDs from household LED lamps as a function of CCT. The samples per CCT base class (2700 K, 3000 K, 4000 K, and 6500 K) consisted of different types of SMD LEDs with similar CCTs to provide a more realistic model of targeted recycling.

#### 2.3.1. Combustion of Samples

In order to select the combustion temperature of the organic part of the samples, a solid SMD LED was tested by thermogravimetric analysis (TGA) (Figure 3a) (brand: SETARAM; (Setaram—Research Services, Geneva, Switzerland) Model: TG DTA DSC +1600 °C), and the temperature of 700 °C was selected, based on which porcelain crucibles (brand: JIPO, (Jizerská porcelainka sro, Desná v Jizerských horách I, Czech Republic) shape: middle) were prepared with the heating profile (Figure 3b) and with the combustion profile of the samples (Figure 3c).

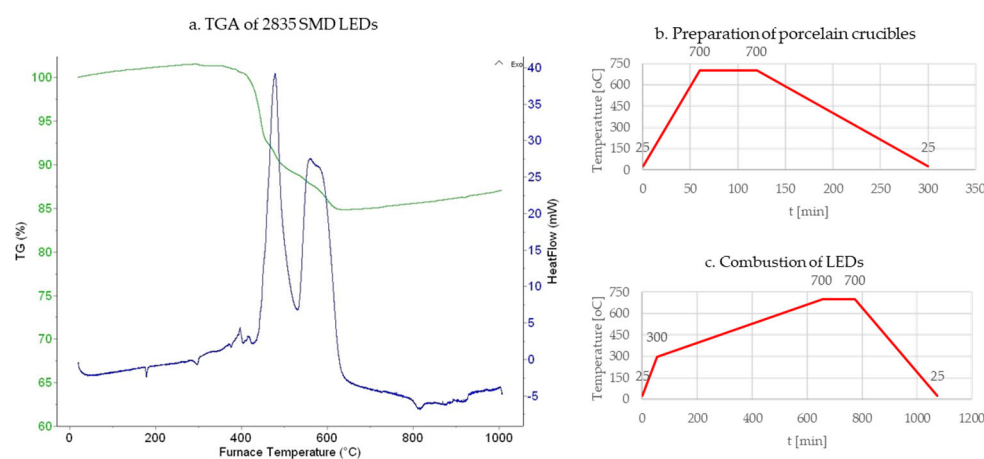


**Figure 3.** (a) Thermogravimetric analysis of a 2835 SMD LED, and temperature and time profiles for crucible preparation (b) and LED combustion (c).

The following equipment were used for the preparation of the crucibles and the combustion of the samples: (a) an analytical balance (brand: KERN (KERN & SOHN GmbH, Balingen, Germany), model: ABP 200-4M),  $d = 0.0001$ ), (b) a laboratory furnace (brand: THERMOLYNE; (THERMOLYNE—ThermoFisher Scientific, Waltham, MA, USA) model: 30400), and a desiccator.

#### 2.3.2. Sample Pulverisation

This step involved the pulverisation of SMD LEDs to produce laboratory samples (quartering—0.1 g per sample) and to make the most effective approach to acids in the samples [126–128] using a ball mill (brand: FRITSCH; (FRITSCH (FRITSCH GmbH, Idar-Oberstein, Germany) model: pulverisette 6) with a zirconium oxide planetary ball mill tank (brand: FRITSCH; volume: 80 mL) and analytical balance (brand: Sartorius; (Sartorius Lab Instruments GmbH & Co. KG, Goettingen, Germany) model: CP124S,  $d = 0.0001$ ).

#### 2.3.3. ICP-MS Analysis

For the characterisation of LEDs, a different laboratory approach was required to study the determination of PMs, REEs, and technology metals (TMs), depending on the structure and the elements studied, compared with other classical electronic components [31,34,73,129]. For each sample and for the determination of PMs and REEs, the solubilisation was carried out as follows: 0.1 g per dry sample (quartering) was weighed on an analytical balance (brand: Sartorius; (Sartorius Lab Instruments GmbH & Co. KG, Goettingen, Germany) model: CP124S,  $d = 0.0001$ ) and transferred to 100 mL teflon beakers.

Subsequently, 15 mL of concentrated HCl solution, 5 mL of concentrated HNO<sub>3</sub> solution (i.e., 20 mL of aqua regia), and 5 mL of concentrated HF solution were added. The beaker was then placed on a hotplate at 200 °C until the sample evaporated to dryness (1–2 h). Then, while the sample was on the hotplate, 5 mL of concentrated HCl solution was added, followed immediately by a few drops of H<sub>2</sub>O<sub>2</sub> solution. The mixture was foamed and allowed to stand (for several seconds). A few drops of the H<sub>2</sub>O<sub>2</sub> solution were added again, the mixture was allowed to settle, and drops of H<sub>2</sub>O<sub>2</sub> were added a third time. When the mixture settled, it was left on a hotplate to dry. When all the solvent had evaporated, 5 mL of concentrated HCl was added, and the mixture was poured into a 100 mL volumetric flask. The flask was made up to the final volume using ultrapure water. After filtration, the final solution was analysed using ICP-MS for the determination of PMs and RREs. For each sample and for the determination of Ag, solubilisation was carried out as follows. The same procedure was followed under the same conditions until the complete evaporation of the solvent. Then, 5 mL of concentrated HNO<sub>3</sub> was added, followed by transfer to a 100 mL volumetric flask, filtration, and the determination of Ag by ICP-MS.

Samples were analysed by ICP-MS (brand: PerkinElmer; (PerkinElmer, Seer Green, Beaconsfield Buckinghamshire HP9 2FX, UK) model: SCIEX ELAN 6100).

### 3. Results and Discussion

#### 3.1. Participation and Characteristics of the LED Lamps

There are two main reasons why the date of LED lamp manufacturing is essential for recycling. First, the concentrations of LED lamps are linked to the manufacturing technology of the time, and the concentrations of PMs and REEs have changed over time. When considering the parameters described in the study by Sideris et al. (2023) [61], the date of manufacture of the lamps in this study was estimated to be between 2016 and 2021. The initial and random collection of the 10.036 kg sample consisted of 221 LED lamps, which were separated according to the base type (Figure 4) and LED technology (SMD LEDs, filament, COB).



**Figure 4.** Lamp base type: (a) E27, (b) E14, (c) G9, (d) R7S, (e) GU10, and (f) MR16 (GU5.3) (authors' images).

In this study, indicator C (classic) (xxx-C) was added to the type of lamps containing SMD LEDs, while indicator R (retro) (xxx-R) was added to the type of lamps containing filament or COB LEDs. Finally, the percentages of each lamp type in the random sample were as follows: (a) E27 47.9% (E27-C 40.7% and E27-R 7.2%), (b) E14 14.5% (E14-C 10.4% and E14-R 4.1%), (c) G9 12.3% (G9-C 11.8% and G9-R 0.5%), (d) R7S 1.9% (R7S-C 1.4% and R7S-R 0.5%), (e) GU10 20.7% (GU10-C 20.7%), and (f) MR16 2.7% (MR16-C 2.7%). According to Wehbie and Semetey (2022) [129], the proportions of different lamp types in the samples examined in different studies can vary significantly between countries and geographical regions, as well as between people's knowledge and culture. From the initial separation, only lamps with SMD LEDs were selected for this study, followed by a selection of unique lamps (121 pcs) that differed in their electrical and photometric characteristics or brand names. In order to guarantee the objectivity of the sample and to study only the individual lamp masses, selective enrichment was carried out, particularly for G9-C (9 pcs), R7S-C (4 pcs), and MR16-C (10 pcs)—the final sample comprised 144 unique lamps. The number of lamps and the number of brands per lamp type were as follows: E27-C 59 (28), E14-C 23 (6), G9-C 16 (8), R7S-C 7 (4), GU10-C 24 (14), and MR16-C 15 (5). Figure 5 shows the variations in electrical power, luminous flux, and mass as a function of lamp type in this study. It should be noted that the results of the present study refer to "retrofit" LED lamps for use in residential applications.

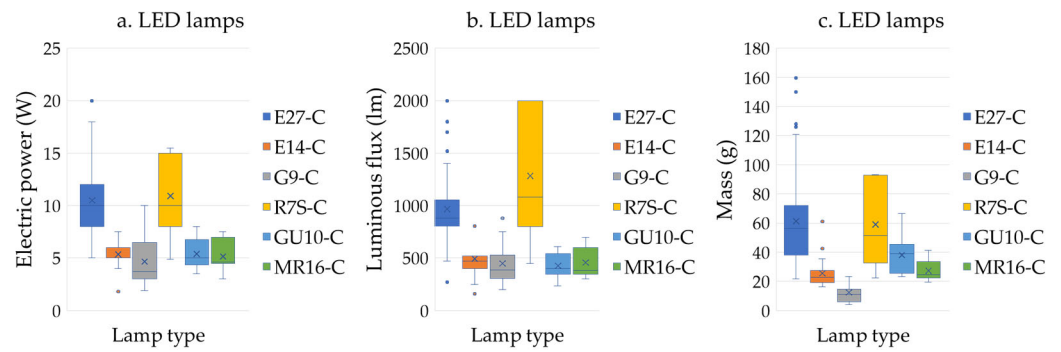


**Figure 5.** Variations in technical characteristics of lamps tested. Where: (.) are the individual extreme values, either minimum or maximum. Where (x) is the average value.

The biological effects of lighting on humans have been observed and studied since ancient times [102]. In particular, illuminance and colour temperature are two critical photometric variables in lighting applications [130] that affect people’s mental states (Kruithof curve) [131,132]. Based on the random sample of lamps in this study, Figure 6 shows people’s preference for the CCT of LED lamps as a function of lamp type and highlights the reduced psychological preference for “cool white” CCT lamps ( $\geq 6000$  K) in residential lighting applications.

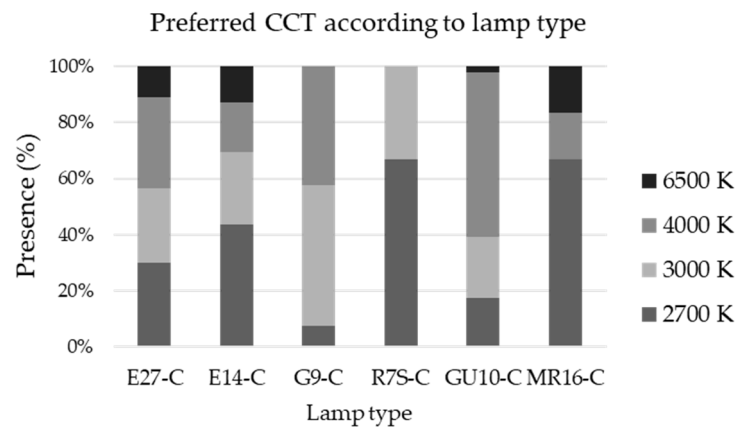


**Figure 6.** The user’s preferred correlated colour temperature, depending on the lamp type.

### 3.2. Individual Structures of LED Lamps with SMD LEDs

As mentioned above, the structure of an LED lamp is more complex than of previous lamp technologies (incandescent and fluorescent lamps). The percentage weight composition of the different basic lamp structures varied considerably. In general, the existing differences can be attributed, individually or in combination, to the following parameters: (a) the manufacturing technology of the respective period, (b) the manufacturing specifications of the brand, and (c) the type of lamp, its electrical power, and the construction material of the body and lens of the lamp (plastic or glass), which change the individual mass percentages of the structural and functional units of the lamps.

#### 3.2.1. LED Module

The “LED module” (Figure 7a) is a specific, and perhaps the most essential, structure of the lamp, both from a functional point of view—the production of luminous flux from LEDs—(Figure 7b) and from a recycling point of view due to the presence of REEs and PMs, as well as base metals (BMs), metals of high economic value, and TMs. After desoldering and removing the LEDs, and in the context of this study, the remaining structure was characterised as a “bare LED module” (Figure 7c). This structure differs significantly from the “LED module” in terms of the presence and concentrations of the group of metals

above [77]. The “bare LED module” corresponds to a “bare PCB” (Figure 7d,e), whose substrate is usually metallic and usually made of aluminium (Figure 7f) and is known as a metal core printed circuit board (MCPCB) [84]. This substrate acts as a heat sink for the structure [133], where the forced thermal equilibrium of an SMD LED is achieved by the “heat sink and heat transfer” structure of the lamp. Depending on the design of the lamp structure, the metal substrate of the LED module can be replaced with flame-retardant (FR) materials such as FR4 [27,51,77,134].



**Figure 7.** (a) “LED module” (E27-C), (b) SMD LEDs, (c) “bare LED module”, (d) top view of the detached PCB, (e) rear view of the detached PCB with the electrical circuit and insulating thin-film coating, and (f) the aluminium substrate of the LED module (authors’ images).

It is worth noting that there are also applications in lamps where LED modules can be of a (a) split type (R7S-C) (Figure 8a), (b) flexible type without a metal substrate or resin (G9-C) (Figure 8b–d), and (c) flexible type with resin material (Figure 8e,f) to be directly bonded to the metal heat transfer and heat sink or onto the ceramic body of the lamp (R7S-C). In addition, in some lamps, the driver and LED module form a single structure (integrated LED system) (Figure 8g) rather than two separate structures [135]. These cases challenge lamp characterisation due to the different components and varying concentrations, especially for PMs, REEs, and other CRMs [77,129].

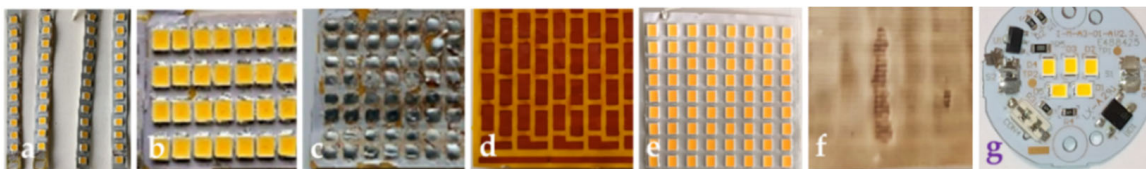


**Figure 8.** Other types of LED modules: (a) split type, (b–d) flexible type without resin, (e,f) flexible type with resin, (g) single-structure type. (Authors’ images.)

The design and dimensions of the LED module, as well as the number, power, and arrangement of LEDs on its surface, are functions of the luminous flux of the lamps and their polar distribution. To achieve these parameters, the design of the LED modules can vary considerably, even for the same type of lamp [122,129]. Figure 9 shows data relating to the analysis of the structure of the LED modules of the lamps examined: in particular, the variation in (a) the mass of the LED module as a percentage of the mass of the lamp (Figure 9a), (b) the number of LEDs as a function of the lamp (Figure 9b), and (c) the total mass of the LEDs as a percentage of the mass of the LED module (Figure 9c). The variation in the number of SMD LEDs as a function of the type of lamp was comparable for the four lamp types and significantly different for the G9-C and R7S-C types. This variation is because these lamp types have a particular construction that contributes to an almost diffuse distribution of luminous flux in the room, requiring many low-luminous-flux SMD LEDs. The percentage of SMD LEDs in the total mass of the LED module varies depending on the number of SMD LEDs and the type of lamp.

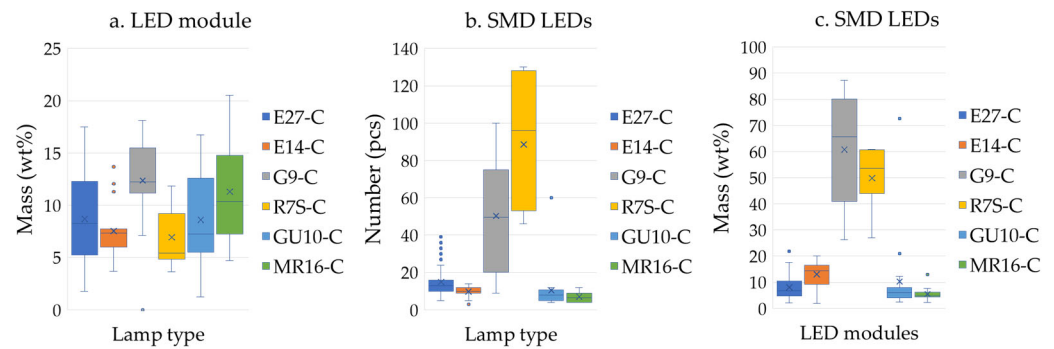


**Figure 9.** Differentiation of the LED module and its components depending on the lamp type in terms of (a) the mass of the LED module as a percentage of the lamp mass, (b) the number of SMD LEDs, and (c) the mass of the SMD LEDs compared to the mass of the LED module. Where: (.) are the individual extreme values, either minimum or maximum. Where (x) is the average value.

### 3.2.2. SMD LEDs

Of the 144 unique LED lamps tested in this study, only 4 used COB LEDs, whereas the rest used SMD LEDs of various types (2835, 3030, 3035, 3528, and 5050). COB LEDs have not been investigated further owing to their low participation and different types. The percentage variation in the mass of waste SMD LEDs in relation to the total mass of each type of lamp studied is shown in Figure 10a, which highlights the significant differentiation of the G9-C and R7S-C lamps compared to the other types, which vary by approximately the same percentage. This difference is due to the desired polar distribution of the luminous flux of these two lamp types, which is achieved with a low luminous flux per SMD LED and an increased number of LEDs. The variation in luminous flux per SMD LED is shown in Figure 10b and is a function of the type of lamp, its electrical power, and the polar distribution of its luminous flux. The variation in mass per waste SMD LED is shown in Figure 10c, from which it can be seen that an average mass value of 0.022 g is acceptable from a recycling perspective.

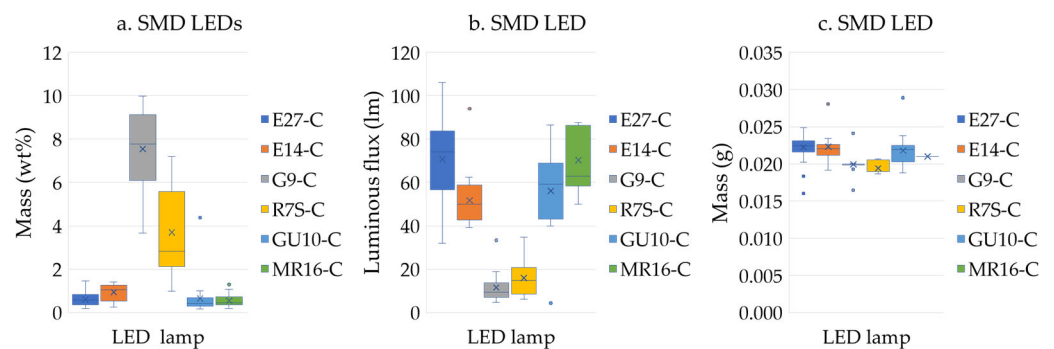


**Figure 10.** Differentiation of SMD LEDs according to the type of lamp in terms of (a) the percentage of their mass contribution to the mass of the lamp, (b) their luminous flux, and (c) the mass of each SMD LED. Where: (.) are the individual extreme values, either minimum or maximum. Where (x) is the average value.

### 3.3. Characterisation of SMD LEDs from LED Lamps via ICP-MS Analysis

Appendix figures show in detail the composition of the samples examined. In particular, (a) Figure A2 shows the participation rate of the SMD LEDs types per CCT, highlighting the high participation rate of type 2835, which ranged between 86 and 100%; (b) Figure A3 shows the participation rate of similar CCTs per basic CCT, highlighting the high participation rate of the basic CCT, which ranged between 60 and 99%; and (c) Figure A4 shows the participation rate of the lamp types as a function of CCT.

The calculated concentrations (mg/kg) of REEs detected by ICP-MS analysis of the tested SMD LEDs of similar CCTs (La, Ce, Eu, Gd, Tb, Lu and Y) are presented in Table 1,

and the results of the literature review on the overall structure of SMD LEDs are also presented in the same table for comparison. The results of the literature review on the presence of REEs in individual masses of SMD LEDs (matrix and encapsulation) are also presented in Table 2. The calculated concentrations (mg/kg) of precious metals detected by ICP-MS analysis of the tested SMD LEDs of similar CCTs (Ag, Au and Pd) are presented in Table 3. The results of the literature review on the overall structure of SMD LEDs are also presented in the same table for comparison. The results of the literature review on the presence of precious metals in individual masses of SMD LEDs (dies and encapsulation) are also presented in Table 4. The results of the present study are supported by the literature review on the overall structure of SMD LEDs and their individual structures (die and encapsulation) and commercially available phosphors.

**Table 1.** Concentration of rare earth elements in SMD LEDs (mg/kg).

Type of LED	SO	AT	La	Ce	Eu	Gd	Tb	Lu	Y	Ref.
SMD	E27-C	ICP-OES		90					6830	[77]
SMD	Tube	"		90					2900	[77]
SMD	Tube	"		100					1800	[51]
SMD	E27-C	"		100					4600	[51]
SMD	E27-C	"		100					12,000	[51]
SMD	E27-C	"		100					5200	[51]
SMD	E27 (pro)	MP-AES		120	89				4590	[122]
SMD	E27 (pro)	"			24				2650	[122]
SMD	E27 (pro)	"		270	120				5410	[122]
SMD	E27 (pro)	"		17	87				3180	[122]
SMD 2835	Tube	ICP-OES		70		70			4040	[73]
SMD 2835-cw	Tube	"		90					5070	[31]
SMD 2835-ww	Tube	"		200					14,250	[31]
SMD 3020	n/a	"		1		0.1			1	[121]
SMD 3810	n/a	"		0.5		0.1			2	[121]
SMD 4014	n/a	"		1		0.1			6	[121]
SMD 5352	n/a	ICP-OES		3		0.1			0.3	[121]
SMD 5630	n/a	"		3		0.1			15	[121]
SMD 5630-1	n/a	"		2		0.1			8	[121]
SMD 5853	n/a	"		2		0.1			6	[121]
SMD 6030	n/a	"		2		0.1			12	[121]
SMD 7020	n/a	"		1		0.1			11	[121]
SMD 7030	n/a	"		2		0.1			10	[121]
SMD COB	n/a	"		0.5		0.1			0.3	[121]
SMD 2700 K	VLLs	ICP-MS	1840	284	69	3.8	0.4	6381	9372	PS
SMD 3000 K	VLLs	"	1287	289	48	3.0	0.1	700	11,551	"
SMD 4000 K	VLLs	"	389	132	29	2.0	0.1	742	4804	"
SMD 6500 K	VLLs	"	242	167	15	1.9	0.1	29	7303	"

n/a (not available), pro (professional use), SO (sample’s origin), AT (analytical technique), VLLs (various LED lamps), ICP-OES (inductively coupled plasma optical emission spectroscopy), MP-AES (microwave plasma atomic emission spectroscopy), PS (present study). Where (“”) indicates the same methodology as the previous one.

**Table 2.** Concentration of rare earth elements in dies and encapsulation (D & E) of SMD LEDs (mg/kg).

Sample	S.O.	A.T.	La	Ce	Eu	Gd	Tb	Lu	Y	Ref.
D & E	SMD LEDs	ICP-MS	≤5	D	320	13	≤5	<100	79,600	[30]
"	"	"	≤5	D	251	6	≤5	154,700	100	[30]
"	"	"	≤5	D	197	15	≤5	100	42,000	[30]
"	"	"	≤5	D	233	9	≤5	<100	48,100	[30]
"	"	"	≤5	D	308	10	≤5	171,900	600	[30]

D (detected). Where (“”) indicates the same methodology as the previous one.

**Table 3.** Concentration of precious metals in SMD LEDs (mg/kg).

Type of LED	S.O.	A.T.	Ag	Au	Pd	Ref.
SMD	n/a	ICP-MS		16		[118]
SMD	E27-C	ICP-OES	4820	520		[77]
SMD	Tube	"	7180	540		[77]
SMD	Tube	"	5900	700		[51]
SMD	E27-C	"	6200	700		[51]
SMD	E27-C	"	3100	200		[51]
SMD	E27-C	"	4400	500		[51]
SMD	E27 (Pro)	MP-AES	780	1210		[122]
SMD	E27 (Pro)	"	1040			[122]
SMD	E27 (Pro)	"	1780	2150		[122]
SMD	E27 (Pro)	"	780	3010		[122]
SMD 2835	Tube	ICP-OES	1660			[73]
SMD 2835-cw	Tube	"	1590	150		[31]
SMD 2835-ww	Tube	"	2390	180		[31]
SMD 3020	n/a	"	349	2265		[121]
SMD 3528	n/a	"	800			[120]
SMD 3528	Strip lights	ICP-MS	2130			[34]
SMD 3810	n/a	ICP-OES	347	3687		[121]
SMD 4014	n/a	"	411	2082		[121]
SMD 5352	n/a	ICP-OES	325	507		[121]
SMD 5630	n/a	"	297	1237		[121]
SMD 5630-1	n/a	"	320	742		[121]
SMD 5853	n/a	"	321	323		[121]
SMD 6030	n/a	"	333	1723		[121]
SMD 7020	n/a	"	340	1171		[121]
SMD 7030	n/a	"	351	939		[121]
SMD COB	n/a	"	1550	875		[121]
n/a	n/a	ICP-AES	1700	90		[26]
SMD 2700 K	VLLs	ICP-MS	5262	934	110	PS
SMD 3000 K	VLLs	"	4754	502	72	"
SMD 4000 K	VLLs	"	3129	677	32	"
SMD 6500 K	VLLs	"	2712	956	63	"

ICP-AES (inductively coupled plasma atomic emission spectroscopy). Where (") indicates the same methodology as the previous one.

**Table 4.** Concentration of precious metals in dies and encapsulation (D & E) of SMD LEDs (mg/kg).

Sample	S.O.	A.T.	Ag	Au	Pd	Ref.
D & E	SMD LEDs	ICP-MS	1589	12	1623	[30]
"	"	"	18	6	4	[30]
"	"	"	977	2	842	[30]
"	"	"	621	4	942	[30]
"	"	"	1377	2	13	[30]
Dies	SMD LEDs	"		1520		[118]

Where (") indicates the same methodology as the previous one.

An essential comparison between the results of this study and the literature review presents insurmountable obstacles related to the sample composition in each case study.

The results of the following studies, individually or in combination, support this statement. H.-T. Lin et al. (2014) reported that the architectural design of LEDs and the composition of their raw materials affect their emission spectrum and, consequently, their luminous flux [95]. X. Ding et al. (2021) pointed out that the depth of the package cavity of SMD LEDs filled by encapsulation varies significantly depending on their type [136], which shapes the geometric dimensions of the encapsulation and distribution profile of the phosphor. According to Tan et al. (2018), the luminous flux of LEDs is a function of the thickness of the resin and the phosphor concentration [108]. According to Y. H. Kim et al. (2015), the “Phosphor/Resin” ratio is significantly different as a function of CCT [101]. According to Kim et al. (2015), the concentration of yellow phosphor in SMD LEDs affects the luminous flux (lm) of SMD LEDs as a function of the sensitivity curve of the human eye [28]. Cenci, Dal Berto, and Castillo et al. (2020) stated that the differences in their concentrations may be due to the electrotechnical characteristics of SMD LEDs, which are a function of the lamp specifications [51]. According to Marwede et al. (2012), there is a significant difference in the total die area per LED lighting product depending on the lighting application [75]. According to Nikulski et al. (2021), the total die area per LED lamp varies depending on the type of lamp and the application in which it is used [76]. According to Cenci, Dal Berto, and Schneider et al. (2020), the number of dies per SMD LED varies depending on the type of lamp [77]. According to Nair et al. (2020), the synergy of inorganic phosphors with appropriate rare-earth ion dopants for each lighting application is a critical component of phosphor-converted LED (pc-LED) structures [109].

When considering (a) the above parameters, (b) the results of the ICP-MS analysis, (c) the percentage of participation of each type of lamp per CCT tested, and (d) the luminous flux per SMD LED and its participation in the sample, it is clarified that, in line with Tunsu et al. (2015) [32] and Balinski et al. (2022) [30], the presence and concentration of REEs in SMD LEDs vary depending on the origin and composition of the sample. In particular, (a) in the case where the sample originates from a specific type of lamp, the presence and concentration of REEs and PMs in SMD LEDs are a function of the electrotechnical specifications of the lamp, and (b) in the case where the sample is formed by the participation of different types of lamps (a more realistic approach from a recycling point of view), an additional factor is taken into account that relates to the percentage participation of each type of lamp in the collected SMD LEDs.

Consequently, the differences between the results of the present study and the literature review may be due, individually or in combination, to the following critical parameters: (a) the type, specifications, and production date of the lamps [30,32]; (b) the composition, origin, and integrity of the sample [113]; (c) the type and photometric characteristics of the sample [28]; and (d) the method of sample characterisation for each case study.

### 3.3.1. Presence of Rare Earth Elements

#### Presence per Element

The detection of REEs by ICP-MS analysis in our samples was related to the presence of a specific phosphor type or the synergy of different phosphor types. In addition to the studies mentioned above, their presence is supported by the commercially available inorganic phosphors used in LEDs for general lighting applications (Table 5).

**Table 5.** Commercially available inorganic phosphors used in LEDs for general lighting applications.

Type	Chemical Formula	Colour	REEs	Brand Name	Ref.
SBCA	$((\text{Sr},\text{Ba})_{10}(\text{PO}_4)_6\text{Cl}_2:\text{Eu}^{2+})$	Blue	Eu	MCC	[137]
CSO	$(\text{CaSc}_2\text{O}_4:\text{Ce}^{3+})$	Green	Ce	MCC	[137]
GYAG	$(\text{Y}_3(\text{Al},\text{Ga})_5\text{O}_{12}:\text{Ce}^{3+})$	"	Ce, Y	MCC	[137]
LuAG	$(\text{Lu}_3\text{Al}_5\text{O}_{12}:\text{Ce}^{3+})$	"	Ce, Lu	MCC, SAM	[137,138]
$\beta$ -SiAlON	$((\text{Si},\text{Al})_3(\text{O},\text{N})_4:\text{Eu}^{2+})$	"	Eu	MCC	[137]

Table 5. Cont.

Type	Chemical Formula	Colour	REEs	Brand Name	Ref.
YGaAG	$Y_3(GaAl)_5O_{12}:Ce^{3+}$	Yellow-green	Ce, Y	SAM	[138]
	$(Y,Gd,Lu)_3(Al,Ga)_5O_{12}:Ce^{3+}$	"	Ce, Gd, Lu, Y		[139]
LSN	$(La_3Si_6N_{11}:Ce^{3+})$	Yellow	La, Ce	MCC	[137]
LYSN	$(La,Y)_3Si_6N_{11}:Ce^{3+}$	"	La, Ce, Y	MCC	[137]
YAG	$(Y_3Al_5O_{12}:Ce^{3+})$	"	Ce, Y	MCC, SAM	[137,138]
	YAG:Ce,Gd	"	Ce, Gd, Y		[140,141]
CASN	$(CaAlSiN_3:Eu^{2+})$	Red	Eu	MCC	[137]
SCASN	$((Sr,Ca)AlSiN_3:Eu^{2+})$	"	Eu	MCC	[137]
	$(CaAlSiN_3:Eu)$	"	Eu	SAM	[138]
	$Y_2O_3:Eu^{3+}$	"	Eu, Y		[142]
	$Y_2O_2S:Eu^{3+}$	"	Eu, Y		[142]

MCC (Mitsubishi Chemical Corporation), SAM (Stanford Advanced Materials). Where ("") indicates the same methodology as the previous one.

In particular, we observed the following:

(a) **Lanthanum (La)**: Lanthanum was also detected in the study by Balinski et al. (2022), where they investigated the “dies and encapsulation” of SMD LEDs, showing a low concentration of  $\leq 5$  mg/kg [30]. In this study, lanthanum was present as a major element (content  $> 0.1\%$ ) for the 2700 K and 3000 K cases and as a trace element (content  $< 0.1\%$ ) for the other CCTs. Its concentration ranged between 242 and 1840 mg/kg, showing a decreasing trend with increasing CCT, and was significantly higher than its concentration in the Earth’s crust (39 mg/kg) [143] and MLCCs from lighting equipment (20 mg/kg) [61].

(b) **Cerium (Ce)**: The combination of the above findings and the grouping of the correlated colour temperatures considered, “warm light” (2700 K and 3000 K) and “cool light” (4000 K and 6500 K), is consistent with the change in cerium concentration, both in the results of the present study and in the results of Vinhal et al. (2022), who studied “warm white” and “cool white” SMD LEDs [31]. The presence of Ce in both the literature review and the present study was as a trace element. Based on the literature review, the concentrations of cerium ranged from 0.5 to 270 mg/kg, while in the study by Balinski et al. (2022), its presence was described as significant. In the present study, the concentration of Ce ranged from 132 to 289 mg/kg, with higher values in the warm CCTs. This concentration is higher than the concentration in the Earth’s crust (66.5 mg/kg) [143] but lower than the concentration in MLCCs from lighting equipment (530 mg/kg) [61].

(c) **Europium (Eu)**: Europium was also found in the study by Illés and Kékesi (2023) [122], where SMD LEDs from E27-C professional lamps were analysed, and in the study by Balinski et al. (2022) [30]. Europium was present as a trace element in the results of the relevant studies and in the present study. In the present study, its concentration ranged between 15 and 69 mg/kg, whereas in the study by Illés and Kékesi (2023) [122], the concentration was between 24 and 120 mg/kg. In the study by Balinski et al. (2022), its concentration ranged between 197 and 320 mg/kg [30] and seemed to be significantly higher than the above-mentioned concentrations because of the specificity of their samples (naturally enriched samples). Both in the present study and the study by Illés and Kékesi (2023) [122], the Eu concentration in the SMD LEDs investigated was significantly higher than the concentration in the Earth’s crust (2 mg/kg) [143].

(d) **Gadolinium (Gd)**: Gadolinium has also been detected in studies by Oliveira et al. (2020) [73], Mandal et al. (2023) [121], and Balinski et al. (2022) [30], which documented its presence in phosphors used in SMD LEDs for general lighting applications. According to “Eurofins”, gadolinium was detected as a dopant in YAG phosphors in a study of LED phosphors [144]. Gadolinium was detected as a trace element in the literature review and the present study. Its concentration in the study by Mandal et al. (2023) [121] was extremely low and of constant value for all the samples considered (0.1 mg/kg), while in the study

by Oliveira et al. (2020) [73], the concentration was high (70 mg/kg). Considering the “enriched samples” examined in the study by Balinski et al. (2022) [30], the concentration of gadolinium ranged between 6 and 13 mg/kg and is higher than the concentration in the present study, which ranges between 1.9 and 3.8 mg/kg. The gadolinium concentration in the present study, compared with its concentration in the Earth’s crust (6.2 mg/kg) [143] shows a lower concentration. A comparison with its concentration in MLCCs from lighting equipment (150 mg/kg) [61] shows a significantly lower concentration.

(e) **Terbium (Tb)**: The terbium concentration in the results of the present study ranged between 0.1 and 0.4 mg/kg, as well as its low presence in the study by Balinski et al. (2022) [30] ( $\leq 5$  mg/kg). The terbium concentration in the waste SMD LEDs in the present study appears to be significantly lower than that in the Earth’s crust (1.2 mg/kg) [143].

(f) **Lutetium (Lu)**: The lutetium concentration in the results of the present study ranged between 29 and 6381 mg/kg and appears to be significantly higher than its concentrations in the Earth’s crust (0.8 mg/kg) [143]. In the present study, lutetium was present as a major concentration at 2700 K, whereas in the other CCTs, it was present as a trace element.

(g) **Yttrium (Y)**: The yttrium concentration per CCT in the examined SMD LEDs ranged between 4804 and 11,551 mg/kg. Except for the concentration of lutetium at 2700 K, its concentration was significantly higher than all the REEs detected. The concentration of yttrium in the samples of the present study compared to the concentration of yttrium (a) in the Earth’s crust (33 mg/kg) [143] is significantly higher; (b) in MLCCs from lighting equipment (2200 mg/kg) [61], it appears higher; and (c) in MLCCs of a specific colour (brown), its value of 3000 mg/kg and 8000 mg/kg [20] are comparable.

#### Group Presence

The concentration of REEs in the samples tested in this study differed significantly between the CCTs (Figure 11a). It ranged between 6098 and 17,950 mg/kg, with the highest concentration at 2700 K and the lowest at 4000 K. Figure 11b shows the percentage contribution of each element per CCT, which ranged as follows: La, 3.119–10.251%; Ce 1.582–2.165%; Eu 0.193–0.476%; Gd, 0.021–0.033%; Tb, 0.001–0.002%; Lu, 0.374–35.548%; and Y, 52.211–94.135%. This figure also highlights the high participation of (a) Y in all CCTs, (b) La in the warm CCTs (2700 K and 3000 K), and (c) Lu at 2700 K.

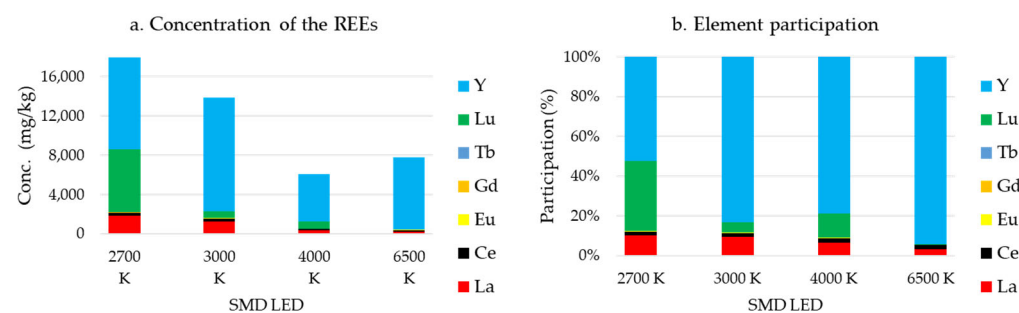


**Figure 11.** Rare earth elements in waste SMD LEDs per CCT: (a) total concentration, (b) percentage participation of each element in the configuration of its stored potential.

In general, the differences in REE concentrations are due to the composition of the sample and its specifications. In particular, and according to the relevant literature below, it is clear that both the presence of REEs and their concentrations can vary significantly depending on the type, CCT, and, more generally, the specifications of SMD LEDs. According to Balinski et al. (2022), among the five different types of SMD LEDs investigated, the masses of “dies and encapsulation” per SMD LED differed significantly [30]. According to Tan et al. (2018), increasing the thickness of the resin and the concentration of phosphor leads to the production of “warm light” [108]. According to Y. H. Kim et al. (2015), in the industrial production of “blue LEDs” with CRI > 90 (high-colour-fidelity lighting applications), the “phosphor to resin” ratio varies as a function of CCT, showing a decreasing

trend in phosphor content with increasing CCT [101], which “matches” the trend of REE concentrations in the present study.

The presence of REEs may be related to specific phosphors, where modifying their chemical composition [139] or the synergy between them [68] contributes to creating the desired luminous flux composition, particularly for SMD LEDs. In particular, we have the following combinations:

(a) The combination of elements Y, Gd, Lu, and Ce may be associated with the presence of the commercial phosphor  $(Y,Gd,Lu)_3(Al,Ga)_5O_{12}:Ce^{3+}$ , where according to Kwangwon Park et al. (2016), through varying its chemical composition, the desired (per application) shifting of the generated radiation within the visible region of the electromagnetic spectrum, particularly between the green and yellow “regions”, is achieved [139].

(b) The combination of La and Ce is probably associated with the presence of the commercial LED phosphor LSN  $(La_3Si_6N_{11}:Ce^{3+})$ , while the combination of the elements La, Y and Ce is probably associated with the presence of the commercial LED phosphor LYSN  $(La,Y)_3Si_6N_{11}:Ce^{3+}$  [137].

(c) The combination of the presence of Y and Ce elements is probably related to the presence of the yellow LED phosphor YAG  $(Y_3Al_5O_{12}:Ce^{3+})$  [45,137,138]. This phosphor, which exhibits high efficiency, is used without the synergy of other phosphors to produce CCT  $\geq 4500$  K [68] because of the absence of “warm” wavelengths [45]. This finding is consistent with the participation of REEs at 6500 K in the present study, where there was an increase in the participation of Y (78.78  $\rightarrow$  94.14) % and the “annihilation” of the participation of Lu (12.17  $\rightarrow$  0.37) % compared to 4000 K, thus producing the desired “cooler” optical effect.

(d) The combination of Lu and Ce is probably related to the presence of the commercially available green phosphor LuAG  $(Lu_3Al_5O_{12}:Ce^{3+})$  [68,137,138], which is used in the production of “white LEDs” [139]. Among other applications, this phosphor is used in combination with yellow or red phosphors [68] to produce “warm” CCTs accompanied by a very high colour rendering index ( $\geq 95$ ). It is exploited in lighting applications where high colour fidelity is required or in special radiation LED applications [65,138]. This combination probably explains the particularly increased presence of Lu (35.55%) at 2700 K compared to the other CCTs, where it ranged between 0.37 and 12.17%.

### 3.3.2. Presence of Precious Metals

#### Presence per Element

In addition to the relevant studies mentioned above, the presence of PMs in the ICP-MS analysis results of this study is also supported by studies of the individual structures of SMD LEDs, as well as the commercially available conductive wires, soldering, and attached die materials used in SMD LEDs designed for general lighting applications. Generally, the presence of precious metals is associated with the raw materials of SMD LEDs and solder residues on their external electrical contacts. In particular, their detection is linked to their possible presence in the power supply of SMD LEDs and internal electrical circuits.

These PMs, individually or in combination, are potentially concentrated in the following locations of the discarded SMD LEDs, particularly (a) in their external electrical contacts (lead frame) [145] and in the solder residues on them [57]; (b) in the electrical contacts of the dies (pads) [51] and in the electrodes of their structure [27,144]; (c) in the electrical connection of the external electrical contacts of the SMD LEDs to the electrical contacts of the dies (wire bonding) and in the electrical connection between the dies in the case of PC-WLEDs that include more than one die in their structure [12,27,28]; (d) in the material of the reflector (certain types of SMD LEDs); and (e) in the material for the mechanical attachment (die attachment) of the die(s) to their substrate [27].

The raw materials of these individual structures, their structure technology (alloy, solid, plated, or flash-coated), and the type of die(s) (lateral, vertical, or flip-chip) constitute the stored potential of PMs in discarded SMD LEDs. In particular, we have the following:

(a) **Silver (Ag)**: The concentration of Ag in the present study ranged between 2712 and 5262 mg/kg, showing a decreasing trend with increasing CCT, which is in agreement with the results of Vinhal et al. (2022), who studied the SMD LEDs of two main categories of CCT: “warm white” and “cool white” [31]. Based on the literature review, its concentration in the individual structures of SMD LEDs ranged between 297 and 7180 mg/kg, while in the study by Balinski et al. (2022), the concentration ranged between 18 and 1589 mg/kg [30]. The concentration of Ag in the SMD LEDs used in the present study is presented as follows: (a) significantly higher than its concentration in the Earth’s crust (0.075 mg/kg) [146]; (b) comparable to that of MLCCs from both lighting equipment (4670 mg/kg) and various other WEEE (1300–50,100 mg/kg) [61]; (c) comparable to that in Ta capacitors (4600–30,000 mg/kg) [54,61] and integrated circuits (ICs) and diodes (up to 10,000 mg/kg) [54]; and (d) higher than the concentrations of drivers (50–140 mg/kg) and bare LED modules (20–40 mg/kg) of LED lamps (tube, E27-C) [77].

(b) **Gold (Au)**: In the context of the present study, its concentration ranged between 502 and 956 mg/kg, with its highest value at 6500 K. Based on the relevant literature, the concentration of Au in individual structures of SMD LEDs ranged between 150 and 3687 mg/kg, while in the study of their individual structures, its concentration varied: (a) in the study by Balinski et al. (2022), it was between 2 and 12 mg/kg [30]; and (b) in the study by Zhan et al. (2015), where only dies were examined, the concentration was found to be 1520 mg/kg [118]. The concentration of Au in the present study compared to (a) its concentration in the Earth’s crust (0.0032 mg/kg) [146] is significantly higher; (b) that in MLCCs from both lighting equipment (10 mg/kg), it is significantly higher, while from various other WEEEs (1–10,000) mg/kg [61], it is comparable; (c) that in ICs, transistors, and diodes (up to 10,000 mg/kg) [54], it is lower; (d) the concentrations of drivers (140–200 mg/kg) and bare LED modules (280–300 mg/kg) of LED lamps (tube, E27-C) [77], it ranges from comparable to higher.

(c) **Palladium (Pd)**: The detection of Pd in the present study is also supported by the study of Balinski et al. (2022), who examined the individual structures of SMD LEDs (dies and encapsulation) [30], which, as expected, included the solder wire. In addition, its detection is supported by commercially available solder wires used in microelectronics in general and SMD LEDs in particular [63,87]. In the present study, the concentration of Pd ranged between 32 and 110 mg/kg, showing a continuous decrease in concentration with increasing CCT from 2700 K to 4000 K, while it showed a similar concentration at 3000 K and 6500 K. The concentration of Pd as a function of CCT is shown to be significantly higher than its concentration in the Earth’s crust (0.0082 mg/kg) [146], while it is lower than that of MLCCs from both lighting equipment (1050 mg/kg) and various other WEEEs (500–30,000 mg/kg) [61]. Particularly high concentrations were found in the study by Balinski et al. (2022), particularly in three of the five cases of the examined samples, with a concentration between 842 and 1623 mg/kg, while in the other cases, the concentration was between 4 and 13 mg/kg, which highlights the influence of the technical specifications of SMD LED production on PM concentrations [30]. Even more focused than the study above on the structure of SMD LEDs, Zhan et al. (2015) characterised dies (lateral structure) with gold pads, which showed a high concentration of Au (1520 mg/kg), while no Ag or Pd was detected [118]. This high concentration is probably explained by the specific characteristics of the sample (naturally enriched sample). From the synergy of the two studies above and the study by Alim et al. (2021) [81] related to the use of solder wires containing Pd in their structure, it is clear that the presence of Pd in SMD LEDs is related to the interconnections of their structures (solder wire).

#### Group Presence

The concentration of PMs in the SMD LEDs tested in this study varied significantly per CCT (Figure 12a) and ranged from 3731 to 6305 mg/kg, with the highest concentration at 2700 K and the lowest at 6500 K. Figure 12b shows the percentage contribution of each

element per CCT, which varied for Ag (72.691–89.227%), Au (9.418–25.629%), and Pd (0.821–1.743%), highlighting the high percentage contribution of Ag in all CCTs.

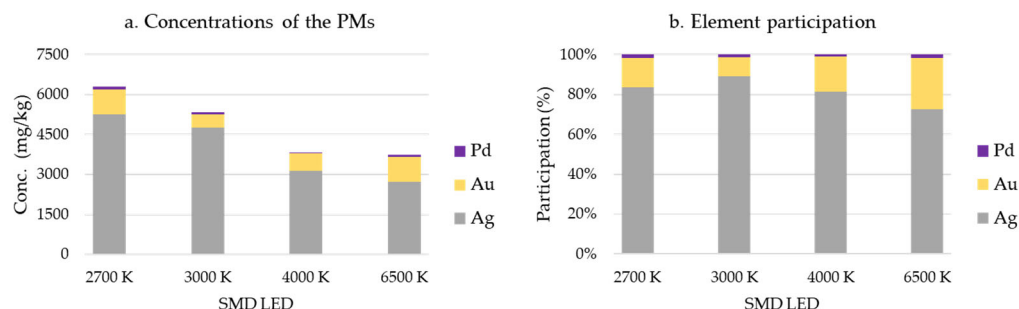


**Figure 12.** Precious metals in waste SMD LEDs per CCT: (a) total concentration, (b) percentage participation of each element in the configuration of its stored potential.

The differences between the concentrations are due to the composition of the sample, both in terms of the type of SMD LEDs and their manufacturing specifications [85,89,147], which are chosen based on techno-economic criteria [63,78,79,81–84,148], and are a function of both the scope of their application [89] and their criticality [78,85].

In particular, the concentrations may vary according to the technical specifications and dimensions of the individual structures of the SMD LEDs, and, in particular, according to (a) the type of SMD LEDs used and the composition of the solder material used on the pads of the LED module; (b) the type of die, its power, its surface area, and the type and composition of the materials used to attach it to the substrate; (c) the type, composition, and geometric dimensions (diameter and length) of the wire; (d) the material used to manufacture the electrical contacts (pads) of the dies; (e) the geometric dimensions of the pads and electrodes of the dies; and (f) the wire reflection coefficient as a function of the CCT [84]. The above-mentioned parameters, individually or in combination, influence the concentrations of precious metals in SMD LEDs.

### 3.4. Concentration of REEs and PMs in Residential LED Lamps

According to Cenci, Dal Berto, and Schneider et al. (2020) [77] and Cenci, Dal Berto, and Castillo et al. (2020) [51], the presence of PMs, such as Ag and Au, in LED lamps is divided into three substructures: (a) drivers, (b) bare LED modules, and (c) SMD LEDs. In particular, according to Cenci, Dal Berto, and Schneider et al. (2020), in LED lamps (tubes and bulbs), the distribution of the aforementioned PMs (Ag, Au) in the lamp structures varied significantly depending on the type of lamp, while the presence of REEs (Ce, Y) was exclusively related to the SMD LED structure [77].

As already explained, REEs in LED lamps are mainly associated with SMD LEDs and MLCCs. Unlike SMD LEDs, MLCCs do not have a constant presence in most types of lamps [61], and their average mass was significantly lower than that of SMD LEDs in this study. This can be explained by the fact that the choice of electronic and non-electronic components of lamp drivers is a function of both their design technology and the lamp's electrical power [114].

In taking into account (a) the average mass of the LED lamp and the average mass of the SMD LEDs per lamp type (Table A1), (b) the percentage of CCT participation per lamp type in the random sample (Table A2), and (c) the precious metal concentrations in the SMD LEDs per CCT, the stored potential of the PMs (Ag, Au, and Pd) in the SMD LEDs of the LED lamps were calculated for an assumed mass of one tonne (1 t) per lamp type (Table A3), as summarised in Figure 13. This figure highlights the strong presence of the G9-C lamp, which is mainly due to both the high mass of the SMD LEDs relative to the total lamp mass (7.549 wt%) and the lamp contribution per CCT, as the concentrations vary significantly as a function of CCT.

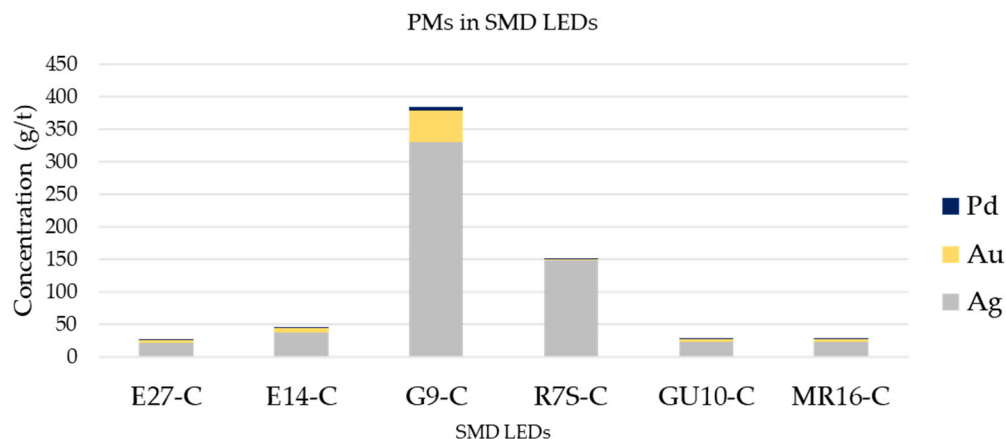


Figure 13. Conditional concentrations of the PMs in SMD LEDs.

In taking into account the above parameters, as well as the presence rate and average mass of MLCCs (Table A4) and the concentrations of REEs in MLCCs from lighting equipment (Table A5), the concentrations of REEs in an assumed mass of one tonne (1 t) per lamp type were calculated and are detailed in Table A6. This table shows the results for the concentrations of REEs and the contribution of SMD LEDs and MLCCs to the concentration of each element. Figure 14 summarises the above-mentioned concentrations. It highlights the superiority of the REE concentration in the G9-C lamp (1099 g/t) compared to the other lamp types, where it varied between 65 and 477 g/t, owing to the significant presence of both SMD LEDs and MLCCs in the structure of this lamp. In general, the differences in concentrations (grammes per tonne of waste LED lamps) between the lamp types are due to (a) the mass of each lamp type; (b) the percentage contribution of the mass of waste SMD LEDs to the total mass of the lamp (wt%); (c) the percentage contribution of each lamp type to the CCTs tested, as the concentration of REEs varies significantly as a function of CCT; and (d) the presence rate, average mass, and concentrations of REEs in MLCCs.

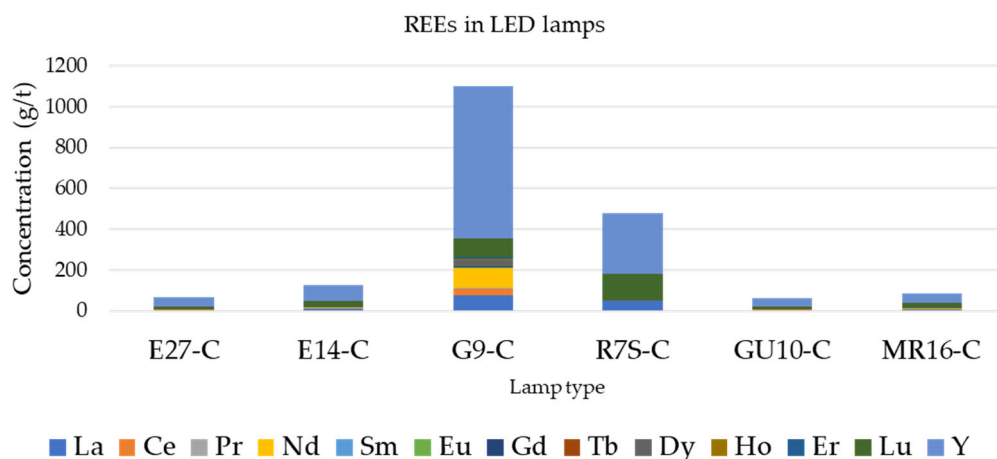


Figure 14. Conditional concentrations of the REEs in LED lamps.

Based on the literature review, the number of studies providing characterisation results on the concentration of REEs and PMs in the overall structure of specific types of LED lamps is minimal. Lim et al. (2013) presented results for an E27 lamp, where Ce corresponds to 7.8 (g/t), Gd to 0.1 (g/t), and Y to 1.7 (g/t) [149]. Tuenge et al. (2013) reported a concentration of Ag of 34 (g/t) under E27 lamps [150]. The differences between the above-mentioned concentrations and the results of the present study are probably due to the type of sample, the year of manufacture of the lamp, and the methodology used in each case study.

#### 4. Conclusions

This study investigated the concentrations of rare earth elements and precious metals in waste SMD LEDs as a function of their correlated colour temperature (2700 K, 3000 K, 4000 K, and 6500 K) using ICP-MS analysis. This study focused on a mixture of waste SMD LEDs removed from a random sample of LED lamps (E27, E14, G9, R7S, GU10, and MR16) used in residential lighting applications. In addition, and as a function of lamp type, issues related to (a) the individual masses of LED modules and SMD LEDs, (b) the conditional characterisation of the above lamp types in terms of the stored potential of REEs (g/t), and (c) the contribution of SMD LEDs to the stored potential of lamp PMs (g/t) were considered.

It was found that in all CCTs, there was a common presence of both REEs (La, Ce, Eu, Gd, Tb, Lu, and Y) and PMs (Ag, Au, and Pd), but with variation in their concentrations as a function of CCT. The main concentrations in SMD LEDs show (a) Ag and Y at all CCTs with values between 2712 and 5262 mg/kg and between 4804 to 11,551 mg/kg, respectively, and (b) La only at “warm” CCTs (2700 K and 3000 K) with values between 1287 and 1840 mg/kg and Lu at 2700 K with 6381 mg/kg. The remaining elements presented as trace elements. According to the individual concentrations per element, the concentrations of both REEs (6098–17,950 mg/kg) and PMs (3731–6305 mg/kg) differ significantly as a function of CCT, and both showed the highest concentration at 2700 K.

Based on the average mass of SMD LEDs relative to the mass of the lamp, the ranking of the six lamp types tested was as follows, in descending order: G9-C (7.55 wt%), R7S-C (3.70 wt%), E14-C (0.94 wt%), GU10-C (0.65 wt%), E27-C (0.61 wt%), and MR16-C (0.56 wt%). The conditional concentrations of REEs per lamp type differed significantly among them. They were enriched in terms of the number of elements (Pr, Nd, Sm, Dy, Ho, and Er) owing to the participation of MLCCs. On the recycling side, the ranking of the lamps in terms of REEs concentrations is, in descending order, G9-C (1098.8 g/t), R7S-C (1098.8 g/t), E14-C (127.3 g/t), MR16-C (84.8 g/t), E27-C (67.4 g/t), and GU10-C (64.8 g/t). The conditionally stored potential of PMs (Ag, Au, and Pd) in the lamp types examined, due to the presence of SMD LEDs, was between 22.189 and 329.997 g/t for Ag, between 2.211 and 48.972 g/t for Au, and between 0.279 and 4.662 g/t for Pd, with the G9-C lamp having the highest concentration of all PMs.

The identification of REEs in specific lamp components (SMD LEDs and MLCCs) and their significantly higher concentrations addresses the need for simpler recycling streams support targeted recycling and, in particular, the selective removal and separate recycling of SMD LEDs. When considering (a) the extremely limited number of studies on the concentrations of REEs and PMs in lamps, (b) the interest of the scientific community in the characterisation of LEDs, and (c) the need to reduce or eliminate the environmental impact when estimating the concentrations of REEs in LED lamps, we believe that it would be acceptable and easier to express the concentrations of Lanthanides, Y, and Pd as a function of the individual masses of the components above in which their presence has been identified, based on the literature. Finally, the results suggest the selective removal of SMD LEDs and their separate recycling.

**Author Contributions:** Conceptualization, K.M.S. and P.S.; methodology, K.M.S., D.F. and V.N.S.; validation, I.K., V.N.S. and D.F.; formal analysis, K.M.S.; investigation, K.M.S.; resources, D.F. and V.N.S.; data curation, K.M.S. writing—original draft preparation, K.M.S. writing—review and editing, P.S., I.K., D.F. and V.N.S.; visualization, K.M.S.; supervision, P.S. and V.N.S.; project administration, P.S. All authors have read and agreed to the published version of the manuscript.

**Funding:** This research received no external funding and the APC was funded by Special Account for Research of ASPETE through the funding programme “Strengthening ASPETE’s research”.

**Data Availability Statement:** Data are contained within the article: The original contributions presented in this study are included in the article. Further inquiries can be directed to the corresponding author.

**Acknowledgments:** Special thanks go to the following: 1. the recycling company “AEGEAN RECYCLINGFOUNDRIES S.A.” for supplying LED lamps; 2. Ioanna Kyriopoulou from the Laboratory of Materials and Environmental Chemistry P.P.C. S.A. for assistance with the use of equipment and useful discussions; 3. Nikolaos Xirokostas and Olga Chalkiadaki, from the Analytical Laboratories Department of the Hellenic Geological and Mineral Exploration Authority (Greece—Attica), for assistance with the use of equipment, the ICP-MS analysis of samples, and useful discussions; and 4. Vassilis Skounakis, Vassilis Orfanos, and Konstantinos Liogas for useful discussions. Authors K. Sideris, I. Katsiris, D. Fragkoulis, V. Stathopoulos, and P. Sinioros acknowledge the financial support for the dissemination of this work from the Special Account for Research of ASPETE through the funding programme “Strengthening ASPETE’s research”.

**Conflicts of Interest:** The authors declare that they have no known competing financial interest or personal relationships that could have influenced the work reported in this study.

### Nomenclature

BMs	base metals
CCT	corelated colour temperature
CMW-LED	colour mixing white LED
COB	chip on board
CRI	colour rendering index
CRMs	critical raw materials
CW	cool white
EI	economic importance
FR	flame retardant
HID	high-intensity discharge
ICP-MS	inductively coupled plasma mass spectrometry
IR-LEDs	infrared LEDs
LED	light-emitting diode
MCPCB	metal core printed circuit board
MLCCs	multi-layer ceramic capacitors
n-ZEB	near-zero energy buildings
PCB	printed circuit board
PC-WLED	phosphor-converted white LED
PGMs	platinum group metals
PiS	phosphor in silicon
PMs	precious metals
REEs	rare earth elements
SEM-EDX	scanning electron microscopy with energy dispersive X-ray spectroscopy
SMD	surface-mount device
SR	supply risk
SSL	solid-state lighting
TMs	technology metals
UV-LEDs	ultraviolet LEDs
V-LEDs	visible LEDs
WEEE	waste electrical and electronic equipment
WW	warm white
ZEB	zero-energy buildings

Appendix A

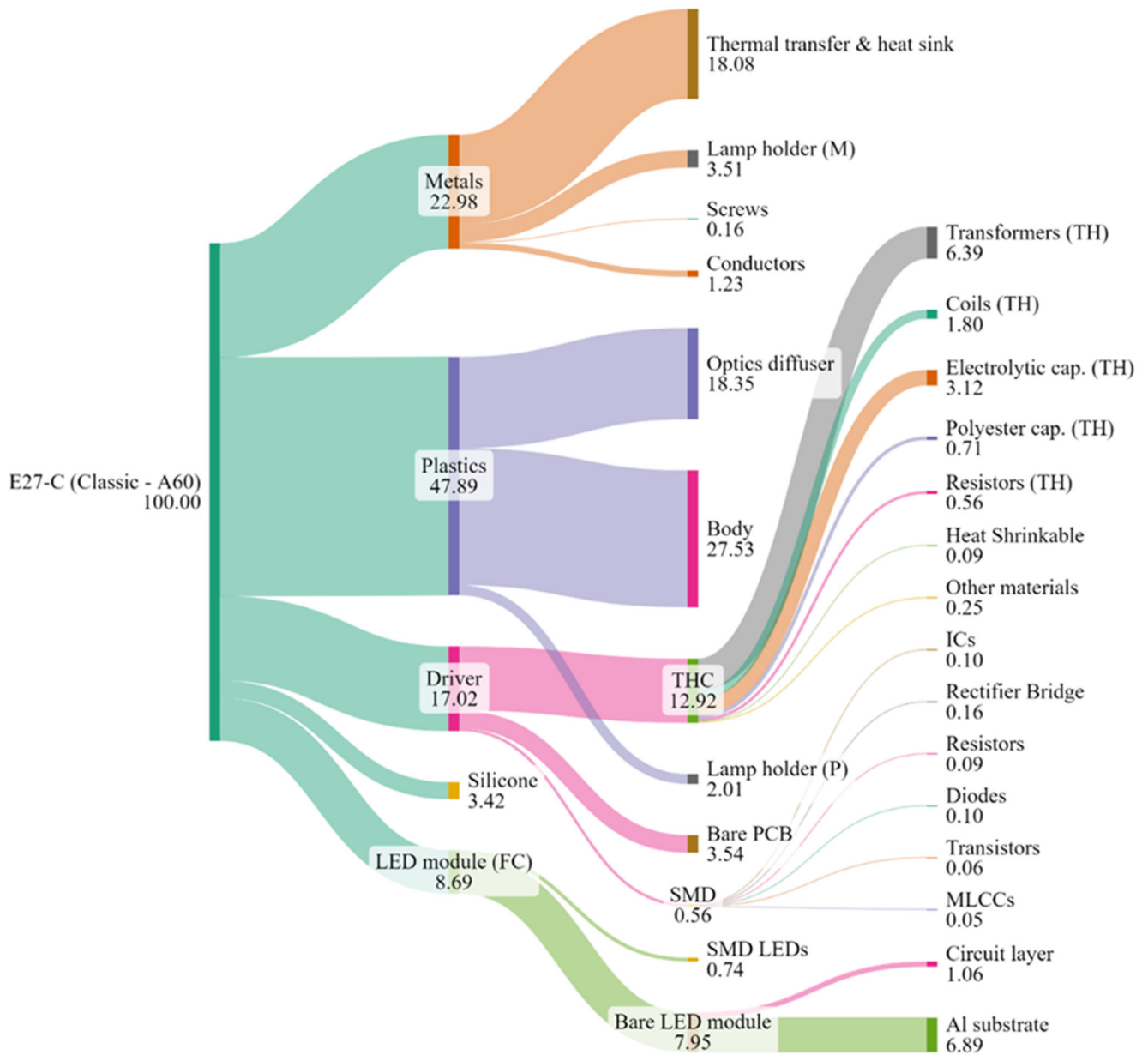


**Figure A1.** Sankey diagram of the average percentage analysis of the individual components of an E27-C LED lamp (Classic-A60) in relation to the total mass of the lamp (wt%). Made at SankeyMATIC.com (accessed on 28 December 2023). SMD—surface-mount device; TH—through-hole.

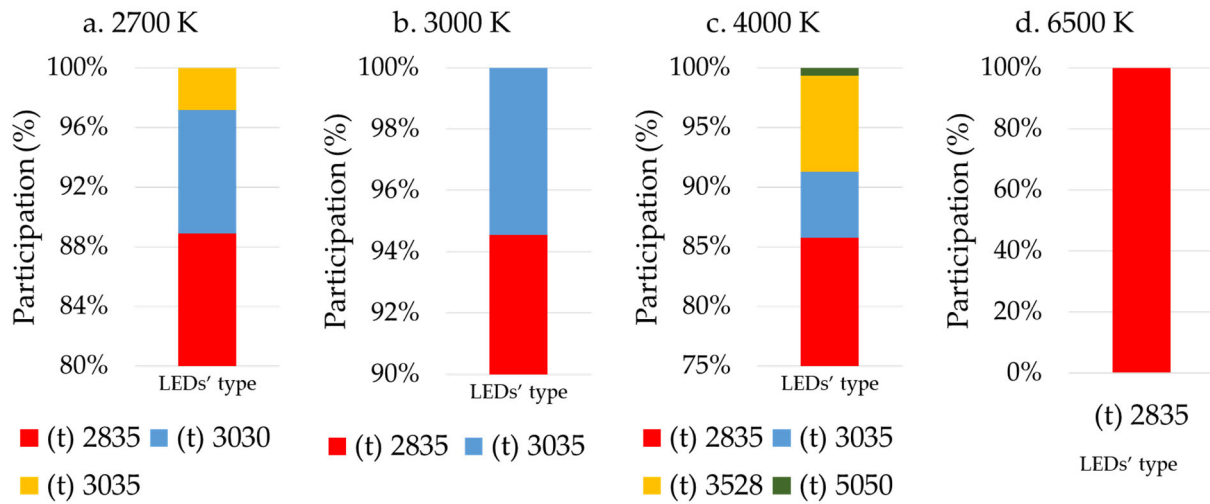


Figure A2. Participation of different types of SMD LEDs per correlated colour temperature.

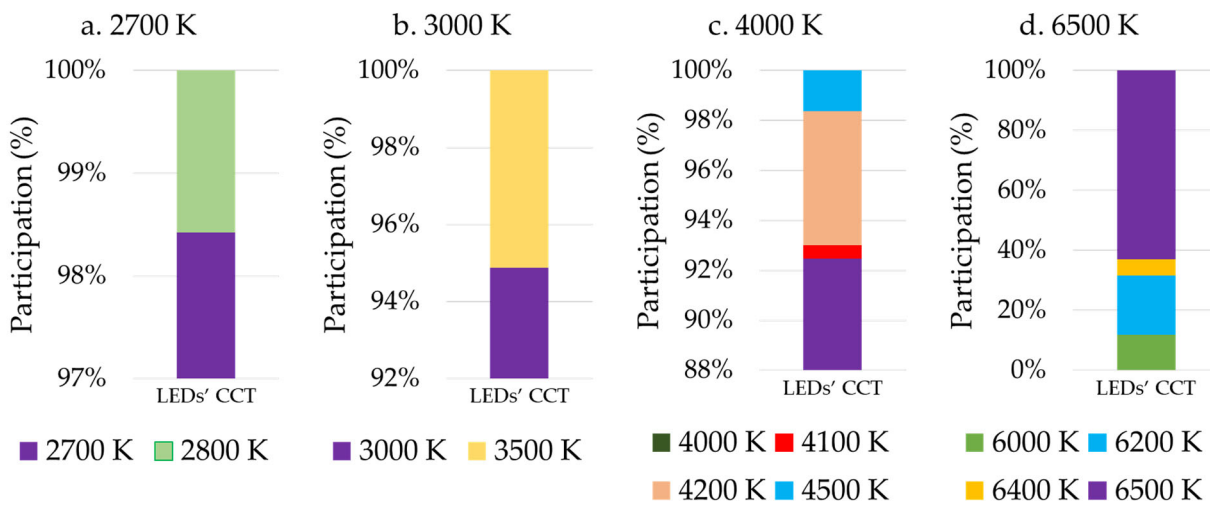


Figure A3. Participation of closely related correlated colour temperatures in the most common choice of each case studied.

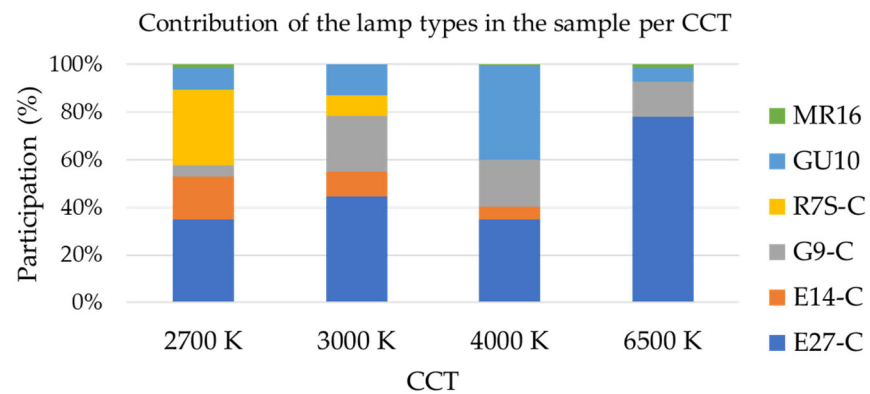


Figure A4. Percentage of each lamp type in the sample per correlated colour temperature tested.

**Table A1.** Average mass (g) of LED lamp and SMD LEDs by lamp type.

Lamp Type	E27-C	E14-C	G9-C	R7S-C	GU10-C	MR16-C
LED lamps	61.250	25.630	12.354	59.108	38.023	27.412
SMD LEDs	0.327	0.219	0.993	1.719	0.234	0.143

**Table A2.** Participation (%) of LED lamps in the random sample per CCT.

CCT	E27-C	E14-C	G9-C	R7S-C	GU10-C	MR16-C
2700 K	30.00	43.48	7.69	66.67	17.39	66.67
3000 K	26.67	26.09	50.00	33.33	21.74	0.00
4000 K	32.22	17.39	42.31	-	58.70	16.67
6500 K	11.11	13.04	-	-	2.17	16.67

**Table A3.** Stored potential conditional per element contained in waste SMD LEDs (g per 1 t of lamp).

Type of LED Lamp	Ag	Au	Pd
E27-C	22.189	3.942	0.371
E14-C	37.819	6.660	0.687
G9-C	329.997	48.972	4.662
R7S-C	148.106	2.211	0.279
GU10-C	23.657	4.245	0.338
MR16-C	23.380	4.668	0.465

**Table A4.** Presence (%) and average mass (g) of MLCCs in LED lamps according to their type.

MLCCs	E27-C	E14-C	G9-C	R7S-C	GU10-C	MR16-C	Ref.
Presence	66	65	100	100	48	100	[61]
Average mass	0.042	0.055	0.328	0.033	0.038	0.034	[61]

**Table A5.** Concentrations of MLCCs from lighting equipment (mg/kg).

	La	Ce	Pr	Nd	Sm	Gd	Dy	Ho	Er	Y	Ref.
MLCCs	20	530	90	3660	50	150	1310	150	230	2200	[61]

**Table A6.** Conditional concentrations (g t<sup>-1</sup>) and distribution (%) of REEs in LED lamps.

	REEs	La	Ce	Pr	Nd	Sm	Eu	Gd	Tb	Dy	Ho	Er	Lu	Y
E27-C	Conc.	5.601	1.433	0.041	1.658	0.023	0.238	0.083	0.001	0.593	0.068	0.104	12.511	45.051
	LEDs	99.84	83.24	Contribution (%) of the components to the concentration of each element										
	MLCCs	0.16	16.76	-	-	-	100	18.01	100	-	-	-	-	100
E14-C	Conc.	10.581	2.821	0.126	5.106	0.070	0.423	0.235	0.002	1.827	0.209	0.321	26.402	78.914
	LEDs	99.74	73.79	Contribution (%) of the components to the concentration of each element										
	MLCCs	0.26	26.21	100	100	100	-	88.99	-	100	100	100	-	100
G9-C	Conc.	76.857	31.931	2.390	97.173	1.328	3.342	4.195	0.010	34.781	3.983	6.107	92.809	743.943
	LEDs	99.31	55.93	Contribution (%) of the components to the concentration of each element										
	MLCCs	0.69	44.07	-	-	-	100	5.06	100	-	-	-	-	100
R7S-C	Conc.	48.162	0.341	0.050	2.042	0.028	0.179	0.186	0.009	0.731	0.084	0.128	130.507	294.906
	LEDs	99.98	74.55	Contribution (%) of the components to the concentration of each element										
	MLCCs	0.02	25.45	100	100	100	-	44.89	-	100	100	100	-	100

Table A6. Cont.

	REEs	La	Ce	Pr	Nd	Sm	Eu	Gd	Tb	Dy	Ho	Er	Lu	Y
GUI10-C	Conc.	5.138	1.444	0.043	1.757	0.024	0.245	0.088	0.001	0.629	0.072	0.110	10.450	44.870
		Contribution (%) of the components to the concentration of each element												
	LEDs	99.81	82.38	-	-	-	100	17.77	100	-	-	-	-	100
	MLCCs	0.19	17.62	100	100	100	-	82.23	-	100	100	100	-	2.35
MRI16-C	Conc.	6.973	1.905	0.112	4.538	0.062	0.278	0.203	0.002	1.624	0.186	0.285	22.863	45.852
		Contribution (%) of the components to the concentration of each element												
	LEDs	99.64	65.50	-	-	-	100	8.20	100	-	-	-	-	100
	MLCCs	0.36	34.50	100	100	100	-	91.80	-	100	100	100	-	5.95

## References

- Rene, E.R.; Sethurajan, M.; Kumar Ponnusamy, V.; Kumar, G.; Bao Dung, T.N.; Brindhadevi, K.; Pugazhendhi, A. Electronic waste generation, recycling and resource recovery: Technological perspectives and trends. *J. Hazard. Mater.* **2021**, *416*, 125664. [[CrossRef](#)] [[PubMed](#)]
- Horta Arduin, R.; Mathieux, F.; Huisman, J.; Blengini, G.A.; Charbuillet, C.; Wagner, M.; Baldé, C.P.; Perry, N. Novel indicators to better monitor the collection and recovery of (critical) raw materials in WEEE: Focus on screens. *Resour. Conserv. Recycl.* **2020**, *157*, 104772. [[CrossRef](#)] [[PubMed](#)]
- Morf, L.S.; Gloor, R.; Haag, O.; Haupt, M.; Skutan, S.; Di Lorenzo, F.; Böni, D. Precious metals and rare earth elements in municipal solid waste—Sources and fate in a Swiss incineration plant. *Waste Manag.* **2013**, *33*, 634–644. [[CrossRef](#)] [[PubMed](#)]
- Xiong, X.; Liu, X.; Yu, I.K.M.; Wang, L.; Zhou, J.; Sun, X.; Rinklebe, J.; Shaheen, S.M.; Ok, Y.S.; Lin, Z.; et al. Potentially toxic elements in solid waste streams: Fate and management approaches. *Environ. Pollut.* **2019**, *253*, 680–707. [[CrossRef](#)] [[PubMed](#)]
- Masara, V.M. The replacement of triodocian lamps by LED in Brazil: A case of environmental and economic sustainability (short review). *MOJ Civ. Eng.* **2019**, *5*, 31–33. [[CrossRef](#)]
- Tesfaye, F.; Lindberg, D.; Hamuyuni, J.; Taskinen, P.; Hupa, L. Improving urban mining practices for optimal recovery of resources from e-waste. *Miner. Eng.* **2017**, *111*, 209–221. [[CrossRef](#)]
- de Oliveira, R.P.; Benvenuti, J.; Espinosa, D.C.R. A review of the current progress in recycling technologies for gallium and rare earth elements from light-emitting diodes. *Renew. Sustain. Energy Rev.* **2021**, *145*, 111090. [[CrossRef](#)]
- Franz, M.; Wenzl, F.P. Critical review on life cycle inventories and environmental assessments of led-lamps. *Crit. Rev. Environ. Sci. Technol.* **2017**, *47*, 2017–2078. [[CrossRef](#)]
- Kumar, A.; Holuszko, M.; Espinosa, D.C.R. E-waste: An overview on generation, collection, legislation and recycling practices. *Resour. Conserv. Recycl.* **2017**, *122*, 32–42. [[CrossRef](#)]
- Mulvaney, D.; Richards, R.M.; Bazilian, M.D.; Hensley, E.; Clough, G.; Sridhar, S. Progress towards a circular economy in materials to decarbonize electricity and mobility. *Renew. Sustain. Energy Rev.* **2021**, *137*, 110604. [[CrossRef](#)]
- Cenci, M.P.; Dal Berto, F.C.; Camargo, P.S.S.; Veit, H.M. Separation and concentration of valuable and critical materials from wasted LEDs by physical processes. *Waste Manag.* **2021**, *120*, 136–145. [[CrossRef](#)] [[PubMed](#)]
- Huang, C.C.; Weng, T.H.; Lin, C.L.; Su, Y.K. Light output, thermal properties and reliability of using glass phosphors in wled packages. *Coatings* **2021**, *11*, 239. [[CrossRef](#)]
- Buechler, D.T.; Zayaykina, N.N.; Spencer, C.A.; Lawson, E.; Ploss, N.M.; Hua, I. Comprehensive elemental analysis of consumer electronic devices: Rare earth, precious, and critical elements. *Waste Manag.* **2020**, *103*, 67–75. [[CrossRef](#)]
- Wani, S.; Majeed, S. Rare-Earth nanomaterials for Bio-Probe applications. *Appl. Biol. Res.* **2017**, *19*, 241. [[CrossRef](#)]
- Cardoso, C.E.D.; Almeida, J.C.; Lopes, C.B.; Trindade, T.; Vale, C.; Pereira, E. Recovery of Rare Earth Elements by Carbon-Based Nanomaterials—A Review. *Nanomaterials* **2019**, *9*, 814. [[CrossRef](#)] [[PubMed](#)]
- Ueberschaar, M.; Geiping, J.; Zamzow, M.; Flamme, S.; Rotter, V.S. Assessment of element-specific recycling efficiency in WEEE pre-processing. *Resour. Conserv. Recycl.* **2017**, *124*, 25–41. [[CrossRef](#)]
- Lukowiak, A.; Zur, L.; Tomala, R.; LamTran, T.N.; Bouajaj, A.; Strek, W.; Righini, G.C.; Wickleder, M.; Ferrari, M. Rare earth elements and urban mines: Critical strategies for sustainable development. *Ceram. Int.* **2020**, *46*, 26247–26250. [[CrossRef](#)]
- Fang, S.; Yan, W.; Cao, H.; Song, Q.; Zhang, Y.; Sun, Z. Evaluation on end-of-life LEDs by understanding the criticality and recyclability for metals recycling. *J. Clean. Prod.* **2018**, *182*, 624–633. [[CrossRef](#)]
- Kumar, A.; Kuppusamy, V.K.; Holuszko, M.; Song, S.; Loschiavo, A. LED lamps waste in Canada: Generation and characterization. *Resour. Conserv. Recycl.* **2019**, *146*, 329–336. [[CrossRef](#)]
- Charles, R.G.; Douglas, P.; Dowling, M.; Liversage, G.; Davies, M.L. Towards Increased Recovery of Critical Raw Materials from WEEE—evaluation of CRMs at a component level and pre-processing methods for interface optimisation with recovery processes. *Resour. Conserv. Recycl.* **2020**, *161*, 104923. [[CrossRef](#)]
- Balaram, V. Rare earth elements: A review of applications, occurrence, exploration, analysis, recycling, and environmental impact. *Geosci. Front.* **2019**, *10*, 1285–1303. [[CrossRef](#)]
- Tansel, B. From electronic consumer products to e-wastes: Global outlook, waste quantities, recycling challenges. *Environ. Int.* **2017**, *98*, 35–45. [[CrossRef](#)] [[PubMed](#)]

23. Ricci, P.C.; Murgia, M.; Carbonaro, C.M.; Sgariotto, S.; Stagi, L.; Corpino, R.; Chiriu, D.; Grilli, M.L. New life of recycled rare earth-oxides powders for lighting applications. *IOP Conf. Ser. Mater. Sci. Eng.* **2018**, *329*, 012002. [[CrossRef](#)]
24. Kumari, R.; Samadder, S.R. A critical review of the pre-processing and metals recovery methods from e-wastes. *J. Environ. Manag.* **2022**, *320*, 115887. [[CrossRef](#)] [[PubMed](#)]
25. Gao, W.; Chen, F.; Yan, W.; Wang, Z.; Zhang, G.; Ren, Z.; Cao, H.; Sun, Z. Toward green manufacturing evaluation of light-emitting diodes (LED) production—A case study in China. *J. Clean. Prod.* **2022**, *368*, 133149. [[CrossRef](#)]
26. Pourhossein, F.; Mousavi, S.M.; Beolchini, F. Innovative bio-acid leaching method for high recovery of critical metals from end-of-life light emitting diodes. *Resour. Conserv. Recycl.* **2022**, *182*, 106306. [[CrossRef](#)]
27. Hamidnia, M.; Luo, Y.; Wang, X.D. Application of micro/nano technology for thermal management of high power LED packaging—A review. *Appl. Therm. Eng.* **2018**, *145*, 637–651. [[CrossRef](#)]
28. Kim, K.H.; Kim, W.H.; Jeon, S.W.; Choi, M.; Bin Song, S.; Kim, J.P. Effects of the optical absorption of a LED chip on the LED package. *Solid. State. Electron.* **2015**, *111*, 166–170. [[CrossRef](#)]
29. Etafo, N.O. Advancements of Lanthanide-doped Phosphors in Solid-state Lighting Applications. *Curr. Phys.* **2024**, *1*, E220124225904. [[CrossRef](#)]
30. Balinski, A.; Recksiek, V.; Stoll, M.; Christesen, C.; Stelter, M. Liberation and Separation of Valuable Components from LED Modules: Presentation of Two Innovative Approaches. *Recycling* **2022**, *7*, 26. [[CrossRef](#)]
31. Vinhal, J.T.; de Oliveira, R.P.; Coleti, J.L.; Espinosa, D.C.R. Characterization of end-of-life LEDs: Mapping critical, valuable and hazardous elements in different devices. *Waste Manag.* **2022**, *151*, 113–122. [[CrossRef](#)] [[PubMed](#)]
32. Tunsu, C.; Petranikova, M.; Gergorić, M.; Ekberg, C.; Retegan, T. Reclaiming rare earth elements from end-of-life products: A review of the perspectives for urban mining using hydrometallurgical unit operations. *Hydrometallurgy* **2015**, *156*, 239–258. [[CrossRef](#)]
33. Tian, X.; Xie, J.; Hu, L.; Xiao, H.; Liu, Y. Waste LEDs in China: Generation estimation and potential recycling benefits. *Resour. Conserv. Recycl.* **2022**, *187*, 106640. [[CrossRef](#)]
34. Zheng, K.; Benedetti, M.F.; Jain, R.; Pollmann, K.; van Hullebusch, E.D. Recovery of gallium (and indium) from spent LEDs: Strong acids leaching versus selective leaching by siderophore desferrioxamine E. *Sep. Purif. Technol.* **2024**, *338*, 126566. [[CrossRef](#)]
35. Xavier, L.H.; Ottoni, M.; Abreu, L.P.P. A comprehensive review of urban mining and the value recovery from e-waste materials. *Resour. Conserv. Recycl.* **2023**, *190*, 106840. [[CrossRef](#)]
36. Ghisi, E.; Stahnke Manorov, T.C.; Niehuns Antunes, L.; Padilha Thives, L. Electricity Savings Due to the Replacement of Fluorescent Lamps with LEDs in Classrooms. *Eur. J. Sustain. Dev.* **2019**, *8*, 64. [[CrossRef](#)]
37. Doulos, L.T.; Kontadakis, A.; Madias, E.N.; Sinou, M.; Tsangrassoulis, A. Minimizing energy consumption for artificial lighting in a typical classroom of a Hellenic public school aiming for near Zero Energy Building using LED DC luminaires and daylight harvesting systems. *Energy Build.* **2019**, *194*, 201–217. [[CrossRef](#)]
38. Zhong, C.; Geng, Y.; Ge, Z.; Rui, X.; Liang, J.; Wei, W. Promoting future sustainable utilization of rare earth elements for efficient lighting technologies. *Environ. Res. Lett.* **2023**, *18*, 074032. [[CrossRef](#)]
39. Chang, M.H.; Das, D.; Varde, P.V.; Pecht, M. Light emitting diodes reliability review. *Microelectron. Reliab.* **2012**, *52*, 762–782. [[CrossRef](#)]
40. Park, K.; Kim, H.; Hakeem, D.A. Photoluminescence properties of Eu 3+ -and Tb 3+ -doped YAIO 3 phosphors for white LED applications. *Ceram. Int.* **2016**, *42*, 10526–10530. [[CrossRef](#)]
41. Li, W.; Ma, N.; Devakumar, B.; Huang, X. Blue-light-excitable broadband yellow-emitting CaGd<sub>2</sub>HfSc(AlO<sub>4</sub>)<sub>3</sub>:Ce<sup>3+</sup> garnet phosphors for white light-emitting diode devices with improved color rendering index. *Mater. Today Chem.* **2022**, *23*, 100638. [[CrossRef](#)]
42. Liu, L.; Keoleian, G.A. LCA of rare earth and critical metal recovery and replacement decisions for commercial lighting waste management. *Resour. Conserv. Recycl.* **2020**, *159*, 104846. [[CrossRef](#)]
43. Morgan Pattison, P.; Hansen, M.; Tsao, J.Y. LED lighting efficacy: Status and directions. *Comptes Rendus Phys.* **2018**, *19*, 134–145. [[CrossRef](#)]
44. Pourhossein, F.; Mousavi, S.M. Enhancement of copper, nickel, and gallium recovery from LED waste by adaptation of *Acidithiobacillus ferrooxidans*. *Waste Manag.* **2018**, *79*, 98–108. [[CrossRef](#)] [[PubMed](#)]
45. Zhu, H.; Lin, C.C.; Luo, W.; Shu, S.; Liu, Z.; Liu, Y.; Kong, J.; Ma, E.; Cao, Y.; Liu, R.-S.; et al. Highly efficient non-rare-earth red emitting phosphor for warm white light-emitting diodes. *Nat. Commun.* **2014**, *5*, 4312. [[CrossRef](#)]
46. Rawat, K.; Vishwakarma, A.K.; Jha, K. Thermally stable Ca<sub>2</sub>Ga<sub>2</sub>SiO<sub>7</sub>:Tb<sup>3+</sup> green emitting phosphor for tricolor w-LEDs application. *Mater. Res. Bull.* **2020**, *124*, 110750. [[CrossRef](#)]
47. Montoya, F.G.; Peña-García, A.; Juaidi, A.; Manzano-Agugliaro, F. Indoor lighting techniques: An overview of evolution and new trends for energy saving. *Energy Build.* **2017**, *140*, 50–60. [[CrossRef](#)]
48. Fan, J.; Mohamed, M.G.; Qian, C.; Fan, X.; Zhang, G.; Pecht, M. Color Shift Failure Prediction for Phosphor-Converted White LEDs by Modeling Features of Spectral Power Distribution with a Nonlinear Filter Approach. *Materials* **2017**, *10*, 819. [[CrossRef](#)]
49. Dzombak, R.; Padon, J.; Salsbury, J.; Dillon, H. Assessment of end-of-life design in solid-state lighting. *Environ. Res. Lett.* **2017**, *12*, 084013. [[CrossRef](#)]
50. Gao, W.; Sun, Z.; Wu, Y.; Song, J.; Tao, T.; Chen, F.; Zhang, Y.; Cao, H. Criticality assessment of metal resources for light-emitting diode (LED) production—A case study in China. *Clean. Eng. Technol.* **2022**, *6*, 100380. [[CrossRef](#)]

51. Cenci, M.P.; Dal Berto, F.C.; Castillo, B.W.; Veit, H.M. Precious and critical metals from wasted LED lamps: Characterization and evaluation. *Environ. Technol.* **2020**, *43*, 1870–1881. [[CrossRef](#)] [[PubMed](#)]
52. D’Adamo, I.; Rosa, P.; Terzi, S. Challenges in waste electrical and electronic equipment management: A profitability assessment in three European countries. *Sustainability* **2016**, *8*, 633. [[CrossRef](#)]
53. European Commission. *Study on the Critical Raw Materials for the EU*; European Commission: Brussels, Belgium, 2023. [[CrossRef](#)]
54. Wu, C.; Awasthi, A.K.; Qin, W.; Liu, W.; Yang, C. Recycling value materials from waste PCBs focus on electronic components: Technologies, obstruction and prospects. *J. Environ. Chem. Eng.* **2022**, *10*, 108516. [[CrossRef](#)]
55. Fischer, A.C.; Forsberg, F.; Lapisa, M.; Bleiker, S.J.; Stemme, G.; Roxhed, N.; Niklaus, F. Integrating MEMS and ICs. *Microsyst. Nanoeng.* **2015**, *1*, 15005. [[CrossRef](#)]
56. Prabakaran, G.; Barik, S.P.; Kumar, B. A hydrometallurgical process for recovering total metal values from waste monolithic ceramic capacitors. *Waste Manag.* **2016**, *52*, 302–308. [[CrossRef](#)]
57. Maurice, A.A.; Dinh, K.N.; Charpentier, N.M.; Brambilla, A.; Gabriel, J.C.P. Dismantling of printed circuit boards enabling electronic components sorting and their subsequent treatment open improved elemental sustainability opportunities. *Sustainability* **2021**, *13*, 10357. [[CrossRef](#)]
58. Liu, Y.; Song, Q.; Zhang, L.; Xu, Z. Behavior of enrichment and migration path of Cu–Ag–Pd–Bi–Pb in the recovery of waste multilayer ceramic capacitors by eutectic capture of copper. *J. Clean. Prod.* **2021**, *287*, 125469. [[CrossRef](#)]
59. Gautam, P.; Behera, C.K.; Sinha, I.; Gicheva, G.; Singh, K.K. High added-value materials recovery using electronic scrap-transforming waste to valuable products. *J. Clean. Prod.* **2022**, *330*, 129836. [[CrossRef](#)]
60. Mir, S.; Dhawan, N. A comprehensive review on the recycling of discarded printed circuit boards for resource recovery. *Resour. Conserv. Recycl.* **2022**, *178*, 106027. [[CrossRef](#)]
61. Sideris, K.M.; Fragoulis, D.; Stathopoulos, V.N.; Sinioros, P. Multi-Layer Ceramic Capacitors in Lighting Equipment: Presence and Characterisation of Rare Earth Elements and Precious Metals. *Recycling* **2023**, *8*, 97. [[CrossRef](#)]
62. Tang, H.; Ye, H.; Wong, C.K.Y.; Leung, S.Y.Y.; Fan, J.; Chen, X.; Fan, X.; Zhang, G. Overdriving reliability of chip scale packaged LEDs: Quantitatively analyzing the impact of component. *Microelectron. Reliab.* **2017**, *78*, 197–204. [[CrossRef](#)]
63. Alim, M.A.; Abdullah, M.Z.; Aziz, M.S.A.; Kamarudin, R. Die attachment, wire bonding, and encapsulation process in LED packaging: A review. *Sens. Actuators A Phys.* **2021**, *329*, 112817. [[CrossRef](#)]
64. Mastrangelo, C.H.; Muller, R.S.; Kumar, S. Microfabricated incandescent lamps. *Appl. Opt.* **1991**, *30*, 868. [[CrossRef](#)]
65. Chen, L.; Lin, C.C.; Yeh, C.W.; Liu, R.S. Light converting inorganic phosphors for white light-emitting diodes. *Materials* **2010**, *3*, 2172–2195. [[CrossRef](#)]
66. Shih, Y.-C.; Kim, G.; You, J.-P.; Shi, F.G. LED Die Bonding. In *Materials for Advanced Packaging*; Springer International Publishing: Cham, Switzerland, 2017; pp. 733–766.
67. Gayral, B. LEDs for lighting: Basic physics and prospects for energy savings. *Comptes Rendus Phys.* **2017**, *18*, 453–461. [[CrossRef](#)]
68. YUJILEDs. Available online: <https://store.yujintl.com/> (accessed on 17 September 2024).
69. Chen, S.H.; Tsai, C.C. SMD LED chips defect detection using a YOLOV3-dense model. *Adv. Eng. Inform.* **2021**, *47*, 101255. [[CrossRef](#)]
70. Rastogi, C.K.; Sharma, S.K.; Sasmal, S.; Pala, R.G.S.; Kumar, J.; Sivakumar, S. Terbium Ion-Mediated Energy Transfer in WO<sub>3</sub>:Tb<sup>3+</sup> and Eu<sup>3+</sup> Phosphors for UV-Sensitized White Light Emission. *J. Phys. Chem. C* **2021**, *125*, 6163–6175. [[CrossRef](#)]
71. Ouhadou, M.; El Amrani, A.; Messaoudi, C.; Ziani, S. Experimental investigation on thermal performances of SMD LEDs light bar: Junction-to-case thermal resistance and junction temperature estimation. *Optik* **2019**, *182*, 580–586. [[CrossRef](#)]
72. U.S. Department of Energy. *2020 LED Manufacturing Supply Chain*; U.S. Department of Energy: Washington, DC, USA, 2021.
73. Oliveira, R.P.; Botelho Junior, A.B.; Espinosa, D.C.R. Characterization of Wasted LEDs from Tubular Lamps Focused on Recycling Process by Hydrometallurgy. In *Energy Technology 2020: Recycling, Carbon Dioxide Management, and Other Technologies*; Springer International Publishing: Berlin/Heidelberg, Germany, 2020; pp. 317–325.
74. UNIT. Available online: <https://www.unit-led.com/> (accessed on 19 July 2024).
75. Marwede, M.; Chancerel, P.; Deubzer, O.; Jordan, R.; Nils, F. Mass Flows of Selected Target Materials in LED Products Project Introduction—Cycling Resources Embedded in Systems Containing Light-emitting Diodes (CycLED). In *2012 Electronics Goes Green 2012+*; IEEE: Berlin, Germany, 2012.
76. Nikulski, J.S.; Ritthoff, M.; von Gries, N. The Potential and Limitations of Critical Raw Material Recycling: The Case of LED Lamps. *Resources* **2021**, *10*, 37. [[CrossRef](#)]
77. Cenci, M.P.; Dal Berto, F.C.; Schneider, E.L.; Veit, H.M. Assessment of LED lamps components and materials for a recycling perspective. *Waste Manag.* **2020**, *107*, 285–293. [[CrossRef](#)] [[PubMed](#)]
78. An, B.; Zhou, H.; Cao, J.; Ming, P.; Persic, J.; Yao, J.; Chang, A. A Review of Silver Wire Bonding Techniques. *Micromachines* **2023**, *14*, 2129. [[CrossRef](#)]
79. Muß, D.; Koch, R. Bonding wire characterization using non-destructive X-ray imaging. *Microelectron. Reliab.* **2023**, *148*, 115177. [[CrossRef](#)]
80. Mazloum-Nejadari, A.; Khatibi, G.; Czerny, B.; Lederer, M.; Nicolics, J.; Weiss, L. Reliability of Cu wire bonds in microelectronic packages. *Microelectron. Reliab.* **2017**, *74*, 147–154. [[CrossRef](#)]
81. Bakar, M.A.; Atiqah, A.; Jalar, A. Review on Corrosion in Electronic Packaging Trends of Collaborative between Academia–Industry. *Sustainability* **2022**, *14*, 15730. [[CrossRef](#)]

82. Chang, C.Y.; Hung, F.Y.; Lui, T.S. Mechanical and Electrical Properties of Palladium-Coated Copper Wires with Flash Gold. *J. Electron. Mater.* **2017**, *46*, 4384–4391. [[CrossRef](#)]
83. Zhang, Y.; Guo, H.; Cao, J.; Wu, X.; Jia, H.; Chang, A. Research Progress of Palladium-Plated Copper Bonding Wire in Microelectronic Packaging. *Micromachines* **2023**, *14*, 1583. [[CrossRef](#)] [[PubMed](#)]
84. Yuan, J.H.; Chuang, T.H. Luminous efficiency of pd-doped ag-alloy wire bonded led package after reliability tests. *Mater. Sci. Forum* **2019**, *960*, 221–230. [[CrossRef](#)]
85. DENO. Available online: <https://denolighting.com/> (accessed on 12 August 2024).
86. JYLED JYLED. Available online: <https://www.szjy-led.com/> (accessed on 25 June 2024).
87. Heraeus Group. Available online: <https://www.heraeus-group.com/en/> (accessed on 18 July 2024).
88. CAPLINQ. Available online: <https://www.caplinq.com/> (accessed on 17 July 2024).
89. Tsai, H.H.; Lee, J.D.; Tsai, C.H.; Wang, H.C.; Chang, C.C.; Chuang, T.H. An innovative annealing-twinned Ag-Au-Pd bonding wire for IC and LED packaging. In Proceedings of the 2012 7th International Microsystems, Packaging, Assembly and Circuits Technology Conference (IMPACT), Taipei, Taiwan, 24–26 October 2012; pp. 243–246. [[CrossRef](#)]
90. Luo, J.; Wang, Y.; Chen, S.; Li, S.; Zhao, Y.; Chen, J.; Hu, Z.; Li, Y.; Wang, H.; Deng, B.; et al. Surface modification of Mg<sub>2</sub>InSbO<sub>6</sub>:Eu<sup>3+</sup> phosphors and applications for white light-emitting diodes and visualization of latent fingerprint. *J. Alloys Compd.* **2022**, *892*, 162049. [[CrossRef](#)]
91. Kumari, S.; Rao, A.S.; Sinha, R.K. Investigations on photoluminescence and energy transfer studies of Sm<sup>3+</sup> and Eu<sup>3+</sup> ions doped Sr<sub>9</sub>Y<sub>2</sub>W<sub>4</sub>O<sub>24</sub> red emitting phosphors with high color purity for w-LEDs. *J. Mol. Struct.* **2024**, *1295*, 136507. [[CrossRef](#)]
92. Gupta, S.K.; Zuniga, J.P.; Abdou, M.; Thomas, M.P.; De Alwis Goonatilleke, M.; Guiton, B.S.; Mao, Y. Lanthanide-doped lanthanum hafnate nanoparticles as multicolor phosphors for warm white lighting and scintillators. *Chem. Eng. J.* **2020**, *379*, 122314. [[CrossRef](#)]
93. Jung, J.-Y. Luminescent Color-Adjustable Europium and Terbium Co-Doped Strontium Molybdate Phosphors Synthesized at Room Temperature Applied to Flexible Composite for LED Filter. *Crystals* **2022**, *12*, 552. [[CrossRef](#)]
94. Zissis, G.; Bertoldi, P.; Serrenho, T. *Update on the Status of LED-Lighting World Market Since 2018*; EUR 30500 EN; Publications Office of the European Union: Luxembourg, 2021; ISBN 978-92-76-27244-1. [[CrossRef](#)]
95. Lin, H.-T.; Tien, C.-H.; Hsu, C.-P.; Horng, R.-H. White thin-film flip-chip LEDs with uniform color temperature using laser lift-off and conformal phosphor coating technologies. *Opt. Express* **2014**, *22*, 31646. [[CrossRef](#)] [[PubMed](#)]
96. Kim, Y.H.; Viswanath, N.S.; Unithrattil, S.; Kim, H.J.; Im, W.B. Review—Phosphor Plates for High-Power LED Applications: Challenges and Opportunities toward Perfect Lighting. *ECS J. Solid State Sci. Technol.* **2018**, *7*, R3134–R3147. [[CrossRef](#)]
97. Shao, C.; Peng, Z.; Yu, B.; Li, Z.; Ding, X. The Detail Study on the Effect of the Flow During The Curing Process of phosphor Particles on the Color Performance. In Proceedings of the 2020 21st International Conference on Electronic Packaging Technology (ICEPT), Guangzhou, China, 12–15 August 2020; pp. 1–4.
98. Ahn, Y.N.; Kim, K.D.; Anoop, G.; Kim, G.S.; Yoo, J.S. Design of highly efficient phosphor-converted white light-emitting diodes with color rendering indices (R<sub>1</sub>–R<sub>15</sub>) ≥ 95 for artificial lighting. *Sci. Rep.* **2019**, *9*, 16848. [[CrossRef](#)]
99. Ryabochkina, P.A.; Egorysheva, A.V.; Golodukhina, S.V.; Khrushchalina, S.A.; Taratynova, A.D.; Yurlov, I.A. Synthesis and photoluminescence properties of novel LaGa<sub>0.5</sub>Sb<sub>1.5</sub>O<sub>6</sub>: Eu<sup>3+</sup>, Dy<sup>3+</sup>, Tb<sup>3+</sup> and BiGeSbO<sub>6</sub>: Eu<sup>3+</sup>, Dy<sup>3+</sup>, Tb<sup>3+</sup> phosphors. *J. Alloys Compd.* **2021**, *886*, 161175. [[CrossRef](#)]
100. Ma, N.; Li, W.; Devakumar, B.; Zhang, Z.; Huang, X. Utilizing energy transfer strategy to produce efficient green luminescence in Ca<sub>2</sub>LuHf<sub>2</sub>Al<sub>3</sub>O<sub>12</sub>:Ce<sup>3+</sup>,Tb<sup>3+</sup> garnet phosphors for high-quality near-UV-pumped warm-white LEDs. *J. Colloid. Interface Sci.* **2021**, *601*, 365–377. [[CrossRef](#)]
101. Kim, Y.H.; Arunkumar, P.; Park, S.H.; Yoon, H.S.; Im, W. Bin Tuning the diurnal natural daylight with phosphor converted white LED—Advent of new phosphor blend composition. *Mater. Sci. Eng. B* **2015**, *193*, 4–12. [[CrossRef](#)]
102. Dutta, P.S. Full Spectrum Phosphors for White LEDs and Virtual Windows for Light and Health Applications. *ECS J. Solid. State Sci. Technol.* **2020**, *9*, 016023. [[CrossRef](#)]
103. Qiao, J.; Zhao, J.; Liu, Q.; Xia, Z. Recent advances in solid-state LED phosphors with thermally stable luminescence. *J. Rare Earths* **2019**, *37*, 565–572. [[CrossRef](#)]
104. Nie, K.; Zhou, R.; Cheng, C.-A.; Duan, X.; Hu, Z.; Mei, L.; Liu, H.; Zhang, Y.; Wang, L.; Wang, H.; et al. Structure, luminescence properties and energy transfer of terbium and samarium co-doped barium based apatite phosphor with tunable emission colour. *Heliyon* **2022**, *8*, e12566. [[CrossRef](#)]
105. Song, X.; Chang, M.H.; Pecht, M. Rare-earth elements in lighting and optical applications and their recycling. *Jom* **2013**, *65*, 1276–1282. [[CrossRef](#)]
106. Lin, Y.C.; Karlsson, M.; Bettinelli, M. Inorganic phosphor materials for lighting. *Top. Curr. Chem.* **2016**, *374*, 374–421. [[CrossRef](#)] [[PubMed](#)]
107. Gupta, I.; Singh, S.; Bhagwan, S.; Singh, D. Rare earth (RE) doped phosphors and their emerging applications: A review. *Ceram. Int.* **2021**, *47*, 19282–19303. [[CrossRef](#)]
108. Tan, C.M.; Singh, P.; Zhao, W.; Kuo, H.-C. Physical Limitations of Phosphor layer thickness and concentration for White LEDs. *Sci. Rep.* **2018**, *8*, 2452. [[CrossRef](#)]
109. Nair, G.B.; Swart, H.C.; Dhoble, S.J. A review on the advancements in phosphor-converted light emitting diodes (pc-LEDs): Phosphor synthesis, device fabrication and characterization. *Prog. Mater. Sci.* **2020**, *109*, 100622. [[CrossRef](#)]

110. Potdevin, A.; Chadeyron, G.; Boyer, D.; Caillier, B.; Mahiou, R. Sol–gel based YAG: Tb 3+ or Eu 3+ phosphors for application in lighting sources. *J. Phys. D Appl. Phys.* **2005**, *38*, 3251–3260. [[CrossRef](#)]
111. Rubinger, R.M.; da Silva, E.R.; Pinto, D.Z.; Rubinger, C.P.L.; Oliveira, A.F.; da Costa Bortoni, E. Comparative and quantitative analysis of white light-emitting diodes and other lamps used for home illumination. *Opt. Eng.* **2015**, *54*, 014104. [[CrossRef](#)]
112. Tucureanu, V.; Matei, A.; Avram, A.M. Synthesis and characterization of YAG:Ce phosphors for white LEDs. *Opto-Electron. Rev.* **2015**, *23*, 239–251. [[CrossRef](#)]
113. Xia, D.; Lee, C.; Charpentier, N.M.; Deng, Y.; Yan, Q.; Gabriel, J.C.P. Drivers and Pathways for the Recovery of Critical Metals from Waste-Printed Circuit Boards. *Adv. Sci.* **2024**, 2309635, e2309635. [[CrossRef](#)]
114. Kumar, K.J.; Bharath Kumar, G.; Kumar, R.S. Harmonic Impacts of Warm and Cool white LED Bulbs. In Proceedings of the 2019 Global Conference for Advancement in Technology (GCAT), Bangaluru, India, 18–20 October 2019. [[CrossRef](#)]
115. Mizanur Rahman, S.M.; Kim, J.; Lerondel, G.; Bouzidi, Y.; Clerget, L. Value retention options in circular economy: Issues and challenges of LED lamp preprocessing. *Sustainability* **2019**, *11*, 4723. [[CrossRef](#)]
116. Limited, C.I.; Kingdom, U. Automated Sorting and Recycling of Waste Lamps Final Report Summary—ILLUMINATE (Automated Sorting and Recycling of Waste Lamps). 2016, pp. 1–18. Available online: <https://cordis.europa.eu/project/id/603667/reporting> (accessed on 18 December 2024).
117. de Moraes, S.L.; da Silva, D.P.; Fredericci, C.; Pedrosa, F.J.B.; Luz, M.S.; Chermont, E.M.; Pachelli, C.A. Chemical analysis of LED bulb components: Strategies for efficient recycling. *Tecnol. Em Metal. Mater. E Mineração* **2024**, *21*, e3042. [[CrossRef](#)]
118. Zhan, L.; Xia, F.; Ye, Q.; Xiang, X.; Xie, B. Novel recycle technology for recovering rare metals (Ga, In) from waste light-emitting diodes. *J. Hazard. Mater.* **2015**, *299*, 388–394. [[CrossRef](#)] [[PubMed](#)]
119. Dodbiba, G.; Oshikawa, H.; Ponou, J.; Kim, Y.; Haga, K.; Shibayama, A.; Fujita, T. Treatment of Spent LED Light Bulbs for Recycling of Its Components: A Combined Assessment in the Context of LCA and Cost-Benefit Analysis. *Resour. Process.* **2019**, *66*, 15–28. [[CrossRef](#)]
120. Zhan, L.; Wang, Z.; Zhang, Y.; Xu, Z. Recycling of metals (Ga, In, As and Ag) from waste light-emitting diodes in sub/supercritical ethanol. *Resour. Conserv. Recycl.* **2020**, *155*, 104695. [[CrossRef](#)]
121. Mandal, S.; Binti Bakaruddin, B.R.; Jeon, S.; Lee, Y.; Kim, K.W. Assessment of the recycling potential of valuable metals by mapping the elemental composition in discarded light-emitting diodes (LEDs). *J. Environ. Manag.* **2023**, *328*, 116900. [[CrossRef](#)]
122. Illés, I.B.; Kékesi, T. A comprehensive aqueous processing of waste LED light bulbs to recover valuable metals and compounds. *Sustain. Mater. Technol.* **2023**, *35*, e00572. [[CrossRef](#)]
123. Zhang, L.; Zheng, Y.; Mao, J.; Wang, S.; Fu, R.; Yang, Y.; Yin, D.; Song, Q.; Chen, Y. Development of an Al<sub>2</sub>O<sub>3</sub> filled composite for the bracket of ultraviolet light-emitting diodes (UV-LEDs). *Opt. Mater.* **2018**, *83*, 356–362. [[CrossRef](#)]
124. Martins, T.R.; Tanabe, E.H.; Bertuol, D.A. Innovative method for the recycling of end-of-life LED bulbs by mechanical processing. *Resour. Conserv. Recycl.* **2020**, *161*, 104875. [[CrossRef](#)]
125. Zhang, Y.; Zhan, L.; Xu, Z. Recycling Ag, As, Ga of waste light-emitting diodes via subcritical water treatment. *J. Hazard. Mater.* **2021**, *408*, 124409. [[CrossRef](#)]
126. Birloaga, I.; Coman, V.; Kopacek, B.; Vegliò, F. An advanced study on the hydrometallurgical processing of waste computer printed circuit boards to extract their valuable content of metals. *Waste Manag.* **2014**, *34*, 2581–2586. [[CrossRef](#)]
127. Niu, B.; Xu, Z. Innovating e-waste recycling: From waste multi-layer ceramic capacitors to Nb–Pb codoped and ag–Pd–Sn–Ni loaded BaTiO<sub>3</sub> nano-photocatalyst through one-step ball milling process. *Sustain. Mater. Technol.* **2019**, *21*, e00101. [[CrossRef](#)]
128. Panda, R.; Dinkar, O.S.; Jha, M.K.; Pathak, D.D. Hydrometallurgical processing of waste multilayer ceramic capacitors (MLCCs) to recover silver and palladium. *Hydrometallurgy* **2020**, *197*, 105476. [[CrossRef](#)]
129. Wehbie, M.; Semetey, V. Characterization of end-of-life LED lamps: Evaluation of reuse, repair and recycling potential. *Waste Manag.* **2022**, *141*, 202–207. [[CrossRef](#)]
130. Güner, T.; Şentürk, U.; Demir, M.M. Optical enhancement of phosphor-converted wLEDs using glass beads. *Opt. Mater.* **2017**, *72*, 769–774. [[CrossRef](#)]
131. Khajehvarnamkhasti, Z.; Dabaghi, E.; Dehghan, H.; Habibi, E. Relationship between Different Levels of Luminance and Color Temperature of LED Lamps on Human Error and Work Speed in Laboratory Conditions. *Int. J. Environ. Health Eng.* **2024**, *13*, 5. [[CrossRef](#)]
132. Liu, T.; Yuizono, T.; Wang, Z.; Gao, H. The influence of classroom illumination environment on the efficiency of foreign language learning. *Appl. Sci.* **2020**, *10*, 1901. [[CrossRef](#)]
133. Ben Abdelmlek, K.; Araoud, Z.; Canale, L.; Charrada, K.; Zissis, G. Optimal substrate design for thermal management of high power multi-chip LEDs module. *Optik* **2021**, *242*, 167179. [[CrossRef](#)]
134. Raypah, M.E.; Devarajan, M.; Sulaiman, F. Evaluation of current and temperature effects on optical performance of InGaAlP thin-film SMD LED mounted on different substrate packages. *Chin. Phys. B* **2017**, *26*, 078503. [[CrossRef](#)]
135. Esteki, M.; Khajehoddin, S.A.; Safae, A.; Li, Y. LED Systems Applications and LED Driver Topologies: A Review. *IEEE Access* **2023**, *11*, 38324–38358. [[CrossRef](#)]
136. Ding, X.; Shao, C.; Peng, Z.; Yu, B.; Li, Z.; Yang, S. Study on Convective Flow Behaviors of Phosphor Particles During Curing Process of Silicone and the Influences on the Optical Performance of White LEDs. *IEEE Trans. Electron. Devices* **2021**, *68*, 2778–2784. [[CrossRef](#)]
137. Mitsubishi Chemical Corporation. Available online: <https://www.mcgc.com/english/index.html> (accessed on 20 May 2024).

138. Stanford Advanced Materials. Available online: <https://www.samaterials.com> (accessed on 25 May 2024).
139. Park, K.; Kim, T.; Yu, Y.; Seo, K.; Kim, J. Y/Gd-free yellow Lu<sub>3</sub>Al<sub>5</sub>O<sub>12</sub>:Ce<sup>3+</sup> phosphor for white LEDs. *J. Lumin.* **2016**, *173*, 159–164. [[CrossRef](#)]
140. Țucureanu, V.; Matei, A.; Avram, A. The effect of the polymeric matrix on the emission properties of YAG-based phosphors. *J. Alloys Compd.* **2020**, *844*, 156136. [[CrossRef](#)]
141. Shi, H.; Zhu, C.; Huang, J.; Chen, J.; Chen, D.; Wang, W.; Wang, F.; Cao, Y.; Yuan, X. Luminescence properties of YAG:Ce, Gd phosphors synthesized under vacuum condition and their white LED performances. *Opt. Mater. Express* **2014**, *4*, 649. [[CrossRef](#)]
142. Xiong, F.B.; Chen, S.D.; Yang, W.B.; Meng, X.G.; Ma, E.; Zhu, W.Z. Novel niobates Y<sub>3</sub>NbO<sub>7</sub>: Ln<sup>3+</sup> (Ln=Pr, Sm) phosphors for warm white LED: Synthesis and luminescent properties. *Opt. Mater.* **2022**, *128*, 112390. [[CrossRef](#)]
143. Milinovic, J.; Rodrigues, F.J.L.; Barriga, F.J.A.S.; Murton, B.J. Ocean-Floor Sediments as a Resource of Rare Earth Elements: An Overview of Recently Studied Sites. *Minerals* **2021**, *11*, 142. [[CrossRef](#)]
144. eurofins. Available online: <https://www.eurofins.com/> (accessed on 16 June 2024).
145. Liu, H.; Zhang, S.; Pan, D.; Tian, J.; Yang, M.; Wu, M.; Volinsky, A.A. Rare earth elements recycling from waste phosphor by dual hydrochloric acid dissolution. *J. Hazard. Mater.* **2014**, *272*, 96–101. [[CrossRef](#)]
146. Laurent, A. Special Issue on Rare Earths. In *Commod. a Glance*; United Nations: New York, NY, USA, 2014; p. 48.
147. Chiang, T.H.; Lin, Y.C.; Chen, Y.F.; Chen, E.Y. Effect of anhydride curing agents, imidazoles, and silver particle sizes on the electrical resistivity and thermal conductivity in the silver adhesives of LED devices. *J. Appl. Polym. Sci.* **2016**, *133*, 43587. [[CrossRef](#)]
148. Chen, K.J.; Hung, F.Y.; Chang, C.Y. A study of the sulfidation behavior on palladium-coated copper wire with a flash-gold layer (Pca) after wire bonding. *Electronics* **2019**, *8*, 792. [[CrossRef](#)]
149. Lim, S.R.; Kang, D.; Ogunseitán, O.A.; Schoenung, J.M. Potential environmental impacts from the metals in incandescent, compact fluorescent lamp (CFL), and light-emitting diode (LED) bulbs. *Environ. Sci. Technol.* **2013**, *47*, 1040–1047. [[CrossRef](#)]
150. Tuenge, J.R.; Hollomon, B.; Dillon, H.E.; Snowden-Swan, L.J. *Life-Cycle Assessment of Energy and Environmental Impacts of LED Lighting Products, Part 3: LED Environmental Testing*; Pacific Northwest National Lab: Richland, WA, USA, 2013. [[CrossRef](#)]

**Disclaimer/Publisher’s Note:** The statements, opinions and data contained in all publications are solely those of the individual author(s) and contributor(s) and not of MDPI and/or the editor(s). MDPI and/or the editor(s) disclaim responsibility for any injury to people or property resulting from any ideas, methods, instructions or products referred to in the content.